

# A Framework For Replica Exchange.

By

Antons Treikalis

A thesis submitted to the

Graduate School-New Brunswick

Rutgers, The State University of New Jersey

In partial fulfillment of the requirements

For the degree of

Master of Science

Graduate Program in Electrical and Computer Engineering

Written under the direction of

Dr. Shantenu Jha

And approved by

---

---

---

---

New Brunswick, New Jersey

September 16, 2016

# Abstract

Replica Exchange (RE) simulations have emerged as an important algorithmic tool for the molecular sciences. Typically RE functionality is integrated into the molecular simulation software package. A primary motivation of the tight integration of RE functionality with simulation codes has been performance. This is limiting at multiple levels. First, advances in the RE methodology are tied to the molecular simulation code for which they were developed. Second, it is difficult to extend or experiment with various RE methods, since expertise in the molecular simulation code is required. We propose the RepEx framework which addresses the aforementioned limitations, while striking the balance between flexibility (any RE scheme) and scalability (several thousand replicas) over a diverse range of HPC platforms. In this thesis is introduced the RepEx framework, the primary contributions of which are: (i) its ability to support different RE schemes independent of molecular simulation codes, (ii) the ability to execute different exchange schemes and replica counts independent of the specific availability of resources, (iii) a runtime system that has first-class support for task- level parallelism, and (iv) provide the required scalability along multiple dimensions.

## Acknowledgements

# Table of Contents

<b>Acknowledgements</b> . . . . .	2
<b>List of Tables</b> . . . . .	6
<b>List of Figures</b> . . . . .	7
<b>1. Introduction</b> . . . . .	1
1.1. Objectives . . . . .	3
1.2. Structure of the dissertation . . . . .	4
<b>2. Background</b> . . . . .	5
2.1. Molecular Dynamics . . . . .	5
2.2. Numerical Integration . . . . .	7
2.3. Replica Exchange Molecular Dynamics . . . . .	8
2.4. Quantum Mechanics/Molecular Mechanics . . . . .	12
2.5. Asynchronous Replica Exchange . . . . .	14
2.6. Multi-dimensional REMD . . . . .	16
2.7. Molecular Simulation Software Packages with Integrated REMD Capability . . . . .	17
2.8. REMD Software Frameworks . . . . .	22
2.9. Pilot Systems . . . . .	25
2.10. RADICAL-Pilot . . . . .	27
<b>3. Requirements</b> . . . . .	29
<b>4. Design</b> . . . . .	31
4.1. Replica Exchange patterns . . . . .	31
4.2. Pilot system . . . . .	32
4.3. Flexible Execution Modes . . . . .	32
4.4. Asynchronous RE algorithm . . . . .	34

<b>5. Implementation</b>	35
5.1. RepEx Modules	35
5.2. Task Execution Diagram	37
5.3. UML Class Diagram	38
5.4. UML Control Flow Diagram	38
5.5. Summary	40
<b>6. Validation</b>	43
<b>7. Performance Optimization</b>	45
7.1. Initial Evaluation	45
7.2. Optimization I	47
7.3. Optimization II	48
7.4. Optimization III	49
7.5. Optimization IV	51
7.6. Optimization V	51
7.7. Summary	52
<b>8. Experiments</b>	53
8.1. Characterization of Overheads	54
8.2. Performance Characterization of 1D-REMD	54
8.3. T-REMD with NAMD engine	56
8.4. M-REMD performance characterization	57
8.5. REMD with Multi-core Replicas	59
8.6. Asynchronous REMD	61
<b>9. Analysis</b>	70
<b>10. Conclusion</b>	73
<b>11. Future Work</b>	74
<b>Bibliography</b>	75
<b>Appendix A. Appendix</b>	80
A.1. Abbreviations	80

A.2. I/O patterns for different types of REMD simulations with Amber MD engine . .	81
--	----

## List of Tables

- 9.1. Comparison of molecular simulation software packages with integrated REMD capability. We characterize each of the seven packages based on 8 features. For each feature we provide a numerical value or a name corresponding to that feature. 71

## List of Figures

2.1. Schematic representation of exchanges between neighboring replicas at different temperatures [12] . . . . .	11
2.2. Energy histograms for a system at five different temperatures [12] . . . . .	12
2.3. Illustration of the QM/MM method. A region, in which a chemical reaction occurs (cannot be described with a force field), is described by quantum mechanical theory. The remainder of the system is modelled using molecular mechanics [? ]. . . . .	12
2.4. Schematic representation of Replica Exchange Patterns: (a) Synchronous (b) Asynchronous. x-axis represents time. Gray squares represent replicas, blue arrows MD phase propagation and green arrows exchange phase propagation. For both phases (MD and exchange), in synchronous pattern exists a global synchronization barrier. In this figure, for synchronous pattern, both MD and exchange are propagated concurrently but this is not a requirement for this pattern. In asynchronous pattern there is no barrier - MD and exchange can be propagated concurrently, meaning while some replicas run MD other replicas might be running exchange. . . . .	15
2.5. Schematic representation of the parameter exchange schema for the three-dimensional REMD. A, B and C are artificial parameters, which are exchanged between replicas belonging to the same group. For the exchange in any given dimension replicas are grouped based on their parameters in other two dimensions. To be grouped together in dimension 1, parameters of replicas in dimensions 2 and 3 must be equal. In this diagram, group sizes in all dimensions are equal to two. Generally, this is not a requirement - group sizes can exceed this number. . . . .	16
2.6. Schematic representation of NAMD parallelization mechanism [15] . . . . .	17
2.7. Information flow in the Amber program suite . . . . .	20



2.8.	RP overview. An application uses the Pilot API to describe pilots (green squares) and units (red circles). The PilotManager instantiates (dash arrow) pilots, the Unit-Manager instantiates (solid arrow) units. Both managers are executed on the user workstation. Pilots are launched (dashed arrows) on resources A and B via SAGA API, an Agent is bootstrapped for each pilot, units are scheduled (solid arrow) to the Agents via MongoDB and executed by the Agents Executer. Boxes color coding: gray for entities external to RP, white for APIs, purple for RPs modules, green for pilots, yellow for modules components. . . . .	27
4.1.	Schematic representation of Execution Mode I. On the x-axis is time. Gray squares represent replicas, blue arrows MD phase propagation and green arrows exchange phase propagation. Both MD and exchange phase for all replicas are performed concurrently. After MD and exchange phase is placed a global barrier, ensuring that all replicas enter next phase simultaneously. . . . .	33
4.2.	Schematic representation of Execution Mode II. On the x-axis is time. Gray squares represent replicas, blue arrows MD phase propagation and green arrows exchange phase propagation. Replicas don't propagate MD and exchange phase concurrently. Batch size for each phase is determined by the number of CPU cores allocated. A global synchronization barrier is present after both MD and exchange phase, ensuring that all replicas enter next phase simultaneously. . . . .	33
5.1.	RepEx task execution diagram. Top gray square represents RepEx package, middle (yellow) square represents RP API and bottom square represents a target resource. The numbered arrows represent control flow. First in Execution Management Module is created a Pilot description, which is then submitted to RPs Pilot Manager (step 1). Pilot Manager launches a Pilot instance on a target resource (step 2). After a Pilot is active, RepEx workload can be submitted for execution. From Execution Management Module to RPs Unit Manager are submitted Compute Units (step 3), which are defined using a Compute Unit Description. Then Unit Manager submits Compute Units for execution to RPs Agent (step 4). . . . .	37
5.2.	UML class diagram. Execution Management Modules are in green boxes. Remote Application Modules are red boxes and Application Management Module is in blue box. . . . .	41
5.3.	UML Control Flow Diagram. . . . .	42

6.1.	Free energy profile of alanine dipeptide backbone torsion at six different temperatures. In all six subplots, the x and y-axes correspond to $\phi$ and $\psi$ torsion angles, respectively. The range of energies is from 0 kcal/mol to 16 kcal/mol while each level in the contour corresponds to a 1 kcal/mol increment. . . . .	44
7.1.	Initial performance results: Decomposition of average simulation cycle time into contributing factors for alanine dipeptide TUU-REMD. All simulation runs are performed on Stampede. . . . .	47
7.2.	Optimization I: remote generation of simulation input files. Decomposition of average simulation cycle time into contributing factors for alanine dipeptide TUU-REMD. All simulation runs are performed on Stampede. . . . .	48
7.3.	Optimization II: remote generation of restraint files and remote determination of exchange partners. Decomposition of average simulation cycle time into contributing factors for alanine dipeptide TUU-REMD. All simulation runs are performed on Stampede. . . . .	49
7.4.	Optimization III: merging of MD simulation tasks with exchange tasks. Decomposition of average simulation cycle time into contributing factors for alanine dipeptide TUU-REMD. All simulation runs are performed on Stampede. . . . .	50
7.5.	Optimization IV: Increasing the number of execution and data staging workers for RP agent. Using a development branch of the latest RP version. Decomposition of average simulation cycle time into contributing factors for alanine dipeptide TUU-REMD. All simulation runs are performed on Stampede. . . . .	51
8.1.	Characterization of overheads: Data times, RepEx overhead and RP overhead. . . . .	55
8.2.	1D REMD experiments with RepEx: weak scaling. Decomposition of average simulation cycle times $T_c$ (in seconds) into MD simulation time and exchange time for umbrella sampling, salt concentration and temperature exchange. For all simulation runs the number of replicas is equal to the number of CPU cores (e.g. 1 core per replica) and both vary from 64 to 1728. All simulation runs are performed on SuperMIC supercomputer. . . . .	56
8.3.	Parallel Efficiency (% of linear scaling) for Temperature Exchange REMD (1D), Salt Concentration REMD (1D) and Umbrella Sampling REMD (1D) using Amber MD engine on SuperMIC supercomputer. . . . .	57

8.4.	Experiments with NAMD engine. Decomposition of average simulation cycle times $T_c$ (in seconds) into MD simulation time and Exchange time for weak scaling scenario. Experiments are performed on SuperMIC supercomputer, using T-REMD. For MD simulation are used single-core replicas. . . . .	58
8.5.	Multi-dimensional REMD experiments with RepEx - weak scaling. TSU-REMD on Stampede using Amber MD engine. For all simulation runs the number of replicas is equal to the number of CPU cores and both vary from 64 to 1728. For all simulation runs are used single-core replicas. In figure is shown decomposition of average simulation cycle times $T_c$ (in seconds) into MD and exchange times. . . . .	59
8.6.	Multi-dimensional REMD experiments with RepEx: strong scaling. TSU-REMD on Stampede using Amber MD engine. Number of replicas is fixed at 1728, but the number of CPU cores is increased from 112 to 1728. For all runs are used single-core replicas. In figure are shown MD simulation and exchange times. RepEx enables users to vary the size of computational resources independently of the simulation size. Allocating more CPUs reduces the $T_c$ . . . . .	60
8.7.	Parallel Efficiency (% of linear scaling) for TSU-REMD on Stampede using Amber MD engine - (a) weak scaling, (b) strong scaling. . . . .	61
8.8.	Multi-core replica experiments using TUU-REMD with Amber engine. MD times for weak scaling scenario. Experiments are performed on Stampede supercomputer. Number of replicas is fixed at 216, but the number of CPUs per replicas is increased from 1 to 64. . . . .	61
8.9.	Execution times for MD tasks when running QM/MM REMD with synchronous RE pattern and using <b>216</b> replicas: times to run Amber (sander) executable (blue line); times to run Amber executable plus times for file staging (red line). For all simulation runs all replicas are running concurrently. All runs are performed on Stampede HPC cluster. . . . .	63
8.10.	Execution times for MD tasks when running QM/MM REMD with synchronous RE pattern and using <b>512</b> replicas: times to run Amber (sander) executable (blue bars); times to run Amber executable plus times for file staging (red bars). For all simulation runs all replicas are running concurrently. All runs are performed on Stampede HPC cluster. . . . .	64

8.11. Execution times for MD tasks when running QM/MM REMD with synchronous RE pattern and using <b>1000</b> replicas: times to run Amber (sander) executable (blue bars); times to run Amber executable plus times for file staging (red bars). For all simulation runs all replicas are running concurrently. All runs are performed on Stampede HPC cluster. . . . .	65
8.12. Execution times for MD tasks when running QM/MM REMD with synchronous RE pattern and using <b>1728</b> replicas: times to run Amber (sander) executable (blue bars); times to run Amber executable plus times for file staging (red bars). For all simulation runs all replicas are running concurrently. All runs are performed on Stampede HPC cluster. . . . .	66
8.13. Utilization for asynchronous and synchronous RE patterns using different replica counts. Utilization is a percentage of maximal (ideal) simulation time. . . . .	67
8.14. Number of crosswalks for 1D T-REMD with synchronous and asynchronous RE patterns. All runs performed on SuperMIC cluster. Runs with synchronous RE pattern (black bars), asynchronous RE pattern with $w = 0.5$ (dark gray bars) and asynchronous RE pattern with $w = 0.1$ (light gray bars) . . . . .	67
8.15. Ratio of crosswalks to simulation time (ns) for 1D T-REMD with synchronous and asynchronous RE patterns. All runs performed on SuperMIC cluster. Runs with synchronous RE pattern (black bars), asynchronous RE pattern with $w = 0.5$ (dark gray bars) and asynchronous RE pattern with $w = 0.1$ (light gray bars) . . . . .	68
8.16. Number of accepted exchanges for 1D T-REMD with synchronous and asynchronous RE patterns. All runs performed on SuperMIC cluster. Runs with synchronous RE pattern (black bars), asynchronous RE pattern with $w = 0.5$ (dark gray bars) and asynchronous RE pattern with $w = 0.1$ (light gray bars) . . . . .	68
8.17. Number of attempted exchanges for 1D T-REMD with synchronous and asynchronous RE patterns. All runs performed on SuperMIC cluster. Runs with synchronous RE pattern (black bars), asynchronous RE pattern with $w = 0.5$ (dark gray bars) and asynchronous RE pattern with $w = 0.1$ (light gray bars) . . . . .	69
A.1. File movement pattern for Amber MD engine: Temperature exchange. . . . .	84
A.2. File movement pattern for Amber MD engine: Umbrella exchange. . . . .	85
A.3. File movement pattern for Amber MD engine: Salt Concentration exchange. . .	86

# Chapter 1

## Introduction

In recent years, a significant progress in understanding the inner workings of biological systems has been made. This progress lead to an unprecedented increase in the amount of data capturing atomic resolution structures and new sequences. Consequently, the significance of the biomolecular simulations increased dramatically. Currently, the protein data bank [1] had 92104 structures stored. In addition, during the last five years, the number of available structures has doubled. Availability of such data provides a solid experimental base for the MD simulations and enables investigation of the relationships between structure and function. Unfortunately, for the majority of proteins only amino-acid sequences are available [2], meaning that to obtain a detailed 3D structure of proteins, protein folding MD simulations must be carried out.

There are several computational challenges associated with protein folding simulations. To perform an accurate and scalable integration, simulation time-step must be around 1 femtosecond ( $1 \text{ fs} = 10^{-15}$  of a second). This is motivated by the fact, that hydrogen atoms in a biomolecule vibrate with a period of approximately 10 fs [2]. Additionally, simulation runtime necessary to observe the desired changes is at the range of microseconds ( $1 \text{ ms} = 10^{-6}$  of a second). Just to allow a protein to relax into the nearest low-energy state an MD simulation must run for at least a couple of nanoseconds ( $1 \text{ ns} = 10^{-9}$  of a second) [2]. Consequently, runtime required for protein folding simulations is approximately in the range from  $1 \times 10^6$  to  $1 \times 10^9$  time-steps.

To minimize the runtime of the MD simulation, requiring millions of time-steps, one must take advantage of the capabilities of modern HPC clusters. For MD simulations, the problem size is typically fixed. This creates a barrier for parallelization of the simulation. Clearly, there is an undeniable benefit in adaptation of other approaches.

The Replica Exchange (RE) [3] is a popular technique to enhance sampling in molecular simulations. Although RE methods were introduced for Monte Carlo methods, their use with MD has grown rapidly.

REMD simulation consists of two phases: one phase is comprised of MD simulations of

$N$  different replicas of the original system, where each replica has different thermodynamic configuration. The other phase involves exchanges of the thermodynamic configurations between replicas using Metropolis-like acceptance criterion. Initially, REMD [4] was used to perform exchanges of temperatures, but has since been extended to perform Hamiltonian Exchange [5], pH Exchange [6] and other exchange types.

Reinforcing the importance of RE, many community MD engines [7, 2, 8], introduced REMD capability. These solutions often demonstrate respectable performance but share some significant limitations, many of which stem from the tight integration of RE method with the MD simulation engine. For example, tight integration results in a significant duplication of effort between “competing” MD engines; what is worse, tight integration results in RE algorithmic innovation that is localized to specific MD engines, making it difficult to propagate the innovation across community codes. MD engines [7, 2, 8] are highly optimized and specialized codes, often requiring tens of person-years of development. Domain scientists are typically unprepared for the full complexity of these MD engines, yet they are the ones most capable of algorithmic and methodological innovation. Furthermore, the number of exchange parameters, order and number of dimensions are typically hard-coded; the tight integration introduces a barrier to methodological advances and extensibility.

This points to the role of a framework that decouples the RE methodology from MD engines as well as manages the complex runtime requirements of multiple concurrent simulations. REMD simulations should also be expressed independent so as to be agnostic to the details of mapping of replicas to underlying resources. Furthermore, a REMD framework should ensure that in the presence of a failure of single replica, the entire set of simulations does not have to be stopped or restarted. These and other reasons reiterate the importance of a framework with an effective runtime system as the number of replicas and time-scales increases.

To address aforementioned challenges, we develop RepEx [9] – a user-level software framework with a runtime system designed to support the requirements of scalable REMD simulations over multiple dimensions. Conceptually, RepEx aims to decouple the implementation of RE algorithm from MD simulation engine. RepEx also decouples the resource management from the REMD algorithm and MD simulation engine specific details.

RepEx relies on RADICAL-Pilot (RP) [10] as a runtime system to perform resource allocation, task scheduling and data movement. Another distinctive feature of RepEx, partly arising from the use of RP, is fault tolerance: RepEx can either continue a simulation in the case of replica failure or can relaunch a failed replica.

The functionality and flexibility come at a performance price, especially when compared to

highly-customized approaches. We carefully characterize the performance “penalty” and argue that it is an acceptable trade-off given the functionality and flexibility enhancements proffered by RepEx. In fact, as we will chronicle, the diversity in algorithms, exchange parameters and dimensionality at adequate scales is unprecedented. The design of RepEx facilitates implementation of new RE algorithms with a wide range of MD engines. The implementation of RepEx supports up to three-dimensional REMD simulations with an arbitrary ordering of available exchange types.

## 1.1 Objectives

This dissertation is aimed at developing a framework for asynchronous Replica Exchange simulations. To achieve this objective the following tasks must be performed:

- Understand and quantify requirements of the REMD simulations software
- Propose and outline a design, which would satisfy identified requirements
- Implement proposed design and motivate implementation decisions
- Verify that the framework meets identified requirements
- Validate that the framework is capable to run REMD simulations

Additionally several specific functionality requirements were identified:

- support for the NAMD MD engine
- support for the AMBER MD engine
- explicit support for both asynchronous and synchronous REMD
- support for temperature, salt-concentration and umbrella exchange for AMBER MD engine
- support for the multi-dimensional REMD simulations

Another objective was to analyze performance and scalability characteristics of the framework on the following HPC systems: Stampede, SuperMIC and Blue Waters.

## 1.2 Structure of the dissertation

There are eleven chapters in this dissertation. In first chapter we provide motivation for this dissertation. We briefly introduce Molecular Dynamics and Replica Exchange simulations. Then we highlight computational and software barriers limiting scientific progress. Additionally, in first chapter are outlined objectives and structure of the dissertation. Second chapter provides background information, needed to appreciate contents of the subsequent chapters. In this chapter we first introduce theoretical background of the Molecular Dynamics and replica exchange Markov Chain Monte Carlo (MCMC) sampling. Next, we motivate the need for asynchronous replica exchange and introduce multi-dimensional replica exchange. Then, we provide an overview of the molecular simulation software packages with integrated replica exchange molecular dynamics (REMD) capability, such as NAMD and Amber. In next section we also discuss some of the REMD software frameworks, which implement REMD algorithm outside of the MD engine. We finalize the background chapter with discussion of pilot systems and RADICAL-Pilot in particular. In chapter three we outline requirements of the REMD software packages. We categorize requirements into three types: functional, performance (scalability) and usability requirements. In chapter four we describe concepts central to the design of RepEx. Next chapter, chapter five, provides implementation details of the RepEx framework. In chapter six is provided validation of the RepEx implementation. This chapter is followed by the performance optimization chapter, in which is described performance optimization strategy utilized to reduce total simulation time. In chapter eight we characterize performance of the RepEx framework for various REMD simulations and provide experimental evidence highlighting differences between synchronous and asynchronous RE. In next chapter we analyze obtained results. In chapter ten are summarized key conclusions, made at the final stage of this endeavor. In last chapter we present some of the directions for the future development of the RepEx.



## Chapter 2

### Background

#### 2.1 Molecular Dynamics

Computer simulations are aimed at understanding the properties of molecules defined by their interactions and structure. Simulation techniques can be broadly divided into two groups: molecular dynamics simulations (MD) and Monte Carlo simulations (MC). Naturally, there are other simulation techniques, but these two are the most popular ones. Unlike other simulation techniques, MD provides an insight into dynamic properties of the system.

Unlike Monte Carlo simulation, Molecular Dynamics simulation of a molecular system acting under potential energy  $U(q)$  involves numerical, step-by-step, solution of the Newton's equations of motion:

$$p_i = \dot{q}_i m_i \quad \dot{p}_i = -\frac{\partial U(q_i)}{\partial q_i} \quad (2.1)$$

Forces  $p_i$  are acting on atoms, and are derived from a potential energy  $U(q^N)$ , where  $q^N = (q_1, q_2, \dots, q_N)$  represents the complete set of atomic coordinates. Consequently, equation 2.11 yields trajectories in the phase space and is a Hamiltonian system.

##### 2.1.1 Hamiltonian Systems

Hamiltonian systems are linear or non-linear systems with particular symmetry, what allows the stability of equilibrium points to be found and the solution curves to be drawn even though actual solutions are not obtained. For Hamiltonian systems the derivatives  $\frac{dq_i}{dt}$  and  $\frac{dp_i}{dt}$  are partial derivatives of a Hamiltonian function  $H$ . Hamiltonian system is defined as:

$$\frac{dq_i}{dt} = \frac{\partial H}{\partial p_i} \quad (2.2)$$

$$\frac{dp_i}{dt} = -\frac{\partial H}{\partial q_i} \quad (2.3)$$

Classical equations of motion form a Hamiltonian system, with Hamiltonian function defined as:

$$H(q, p) = U(q) + K(p) = U(q) + \sum_i \frac{p_i^2}{2m_i} \quad (2.4)$$

where:  $U(q)$  is potential energy  $K(p)$  is kinetic energy

We now show that equations 2.11 form a Hamiltonian system. First we note that:

$$p_i = m_i v_i \quad (2.5)$$

$$\frac{dp_i}{dt} = m_i \frac{dv_i}{dt} \quad (2.6)$$

Next we note that:

$$-\frac{\partial U}{\partial q_i} = F_i(q) \quad (2.7)$$

where  $F$  is a force vector

We now take a derivative of Hamiltonian  $H$  with respect to  $q_i$ :

$$-\frac{\partial H}{\partial q_i} = -\frac{\partial U}{\partial q_i} = F_i(q) = m a_i = m_i \frac{dv_i}{dt} = \frac{dp_i}{dt} \quad (2.8)$$

Next we take a derivative of Hamiltonian  $H$  with respect to  $p_i$ :

$$-\frac{\partial H}{\partial p_i} = \frac{\partial K}{\partial p} = \frac{p_i}{m} = \frac{m_i v_i}{m_i} = v_i = \frac{dq_i}{dt} \quad (2.9)$$

Now we write Hamiltonian system for the classical equations of motion:

$$\dot{p}_i = -\frac{\partial H}{\partial q_i} = F_i(q) \quad \dot{q}_i = \frac{\partial H}{\partial p_i} = \frac{p_i}{m_i} \quad (2.10)$$

### 2.1.2 Phase space

The term **phase space** is often mentioned when molecular dynamics simulations are discussed. A phase space is a  $6N$ -dimensional space in which there is an axis for every coordinate  $q_N$  and for every momentum  $p_N$ . If a system of Cartesian coordinates is used, then for each atom there are  $x, y, z$  and  $p_x, p_y, p_z$  axes.

Consequently we can describe system change over time as a trajectory in phase space. If we are dealing with a classical system, the energy is conserved and the phase space trajectory adheres to a surface of constant energy [? ].

Ergodic systems, which can reach equilibrium, are capable of exploring all parts of phase space, having the same energy. In other words, a trajectory of a system, which is ergodic, will reach all points in phase space on the constant energy hypersurface with equal probability. If given system is not ergodic, some of the phase space points will remain unvisited and as a consequence the system will not be capable to examine the complete constant energy surface [? ].

A **differential volume element** in phase space is a very small region of  $6N$ -dimensional volume that spans differential elements:

$$dq^N dp^N = dx_1 dy_1 \dots dz_N dp_{x,1} dp_{y,1} \dots dp_{z,N} \quad (2.11)$$

**Configuration space** is the subset of phase space corresponding to the  $3N$  variables  $q^N$ .

## 2.2 Numerical Integration

A numerical integrator calculates an approximate solution trajectory of the system of ordinary differential equations given a time-step and initial positions and velocities of the atoms. The most widely used numerical integrators are: the Verlet algorithm [? ], the Leapfrog algorithm [? ] and the Velocity Verlet algorithm [? ].

The Verlet algorithm offers better stability, time-reversibility and area preserving properties with little additional computational cost in comparison to the Euler method. The solution of Newton's equations of motion using the Verlet algorithm is based on a Taylor series expansion. The two updating steps of the Verlet method are:

$$q_i(t + \Delta t) = 2q_i(t) - q_i(t - \Delta t) + \frac{1}{m_i} \frac{\partial U}{\partial q_i}(t) \Delta t^2 \quad (2.12)$$

$$p_i(t) = m_i \frac{(q_i(t + \Delta t) - q_i(t - \Delta t))}{2\Delta t} \quad (2.13)$$

The Verlet Algorithm relies on two previous time steps,  $t$  and  $t - \Delta t$ , to advance the solution forward. One of the problems with the Verlet algorithm, is the fact, that due to potential loss of accuracy when implementing equation 2.12, the final term in the equation tends to be small and this term may be lost in the round-off error.

The Leapfrog algorithm was developed to correct some of the problems associated with the Verlet algorithm. The name of the algorithm comes from the fact, that  $q$  and  $p$  are "leapfrogging" over each other during integration. The two updating steps of the Leapfrog algorithm are:

$$q_i(t + \Delta t) = q_i(t) + \frac{p_i(t + \frac{\Delta t}{2})}{m_i} \Delta t \quad (2.14)$$

$$p_i(t + \frac{\Delta t}{2}) = p_i(t - \frac{\Delta t}{2}) + \frac{\partial U}{\partial q_i}(t) \Delta t \quad (2.15)$$

The two updating steps of the Velocity Verlet algorithm are:

$$q_i(t + \Delta t) = q_i(t) + \frac{p_i(t)}{m_i} \Delta t + \frac{1}{2m} \frac{\partial U}{\partial q_i}(t) \Delta t^2 \quad (2.16)$$

$$p_i(t + \Delta t) = p_i(t) + \frac{\Delta t}{2} \left( \frac{\partial U}{\partial q_i}(t) + \frac{\partial U}{\partial q_i}(t + \Delta t) \right) \quad (2.17)$$

All three numerical integration algorithms produce deterministic dynamical systems, meaning that there is no stochastic element. In addition, because these algorithms are solving a Hamiltonian system, they conserve the total energy [? ]. We define the total energy as:

$$E(q, p) = U(q) + K(p) \quad (2.18)$$

Each of the three algorithms discussed in this section, when used for MD simulation, produces trajectories in a **microcanonical ensemble**: a set of all molecular configurations with constant energy. Due to the rounding errors of computer hardware and the choice of the step-size, the configurations in the trajectories do not have exactly the same energy. The advantage of the algorithms, presented in this section, is their ability to restrain the energy from divergence.

## 2.3 Replica Exchange Molecular Dynamics

While undertaking simulations of complex systems such as proteins, using Molecular Dynamics (MD) or Monte Carlo (MC) methods, it is problematic to obtain accurate canonical distributions at low temperatures [11]. Replica Exchange Markov chain Monte Carlo (MCMC) sampling or Parallel Tempering is a widely used simulation technique, aimed to improve efficiency of MCMC method, while simulating physical systems. This technique was devised as early as 1986 by swendsen1986replicadsen and Wang [3], but Molecular Dynamics version of the method, which is known as Replica-Exchange Molecular Dynamics (REMD) was first formulated by Sugita and sugita1999replicamoto [4] in 1999. Today parallel tempering is applied in many scientific fields including chemistry, physics, biology, materials science and other.

In Parallel Tempering simulations  $N$  replicas of the original system are used to model phenomenon of interest. Typically, each replica can be treated as an independent system and would

be initialized at a different temperature. While systems with high temperatures are very good at sampling large portions of phase space, low temperature systems often become trapped in local energy minima during the simulation [12]. Replica Exchange method is very effective in addressing this issue and generally demonstrates a very good sampling. In RE simulations, system replicas of both higher and lower temperature sub-sets are present. During the simulation they exchange full configurations at different temperatures, allowing lower temperature systems to sample a representative portion of phase space.

It is obvious that running a simulation of  $N$  replicas of the system would require  $N$  times more compute power. Despite that fact, RE simulations are proven to be at least  $1/N$  times more efficient than single temperature simulations. This is achieved by enabling replicas with lower temperatures to sample phase space regions, not accessible for them in case of regular Monte Carlo simulation, even if it would run  $N$  times longer than RE simulation involving  $N$  replicas. In addition to that, RE method can be very efficiently mapped to distributed-memory architectures of HPC clusters.

Implementation details of the mechanism for performing swaps of configurations between replicas significantly influence efficiency of the method. Issues to consider are: how often should exchanges take place, what is the optimal number of replicas, what is the range of temperatures, how much of a compute power should be dedicated to each replica. In addition to that, in order to prevent the growth as  $\sqrt{N}$  of a system with  $N$  replicas, solutions on how to swap only a part of the system are required [12].

It is worth noting that RE simulations may involve tempering of parameters other than temperature. For example, in some cases simulations where chemical potentials are swapped may demonstrate a better efficiency. A special case of RE method is defined by configuration swaps in a multi-dimensional space of order parameters. This is typically referred as multi-dimensional replica exchange. Thanks to better sampling of phase space enabled by the use of RE method, inconsistencies in some widely used force fields were discovered [12]. It is clear now, that RE method has established its important role in testing of new force fields for atomic simulations.

### 2.3.1 Theory of Replica Exchange Markov Chain Monte Carlo (MCMC) sampling

In standard RE simulation each of  $N$  replicas is assigned a different temperature  $T_i$  and  $T_1 < T_2 < \dots < T_N$ . Here  $T_1$  is a temperature of the simulated system. The partition function

of the ensemble is:

$$Q = \prod_{i=1}^N \frac{q_i}{M!} \int dr_i^M \exp[-\beta_i U(r_i^M)] \quad (2.19)$$

where:

$q_i = \prod_{j=1}^M (2\pi m_j k_B T_i)^{3/2}$  is from integrating out the momenta

$m_j$  is the mass of atom  $j$

$r_i^M$  defines the positions of the  $M$  particles in the system

$\beta_i = 1/(k_B T_i)$  is the reciprocal temperature

$U$  is the potential energy or the part of the Hamiltonian that does not involve the momenta

In case if for all conditions a probability of an exchange is equal, the probability what an exchange between replica  $i$  and  $j$  would be accepted is:

$$A = \min \{1, \exp[(\beta_i - \beta_j)(U(r_i^M) - U(r_j^M))]\} \quad (2.20)$$

where:

$j = i + 1$ , meaning that exchanges are attempted between replicas with "neighboring" temperatures

Replica Exchange method facilitates any set of Monte Carlo moves for a single temperature system, where single-system moves take place between exchanges [12]. An example of a typical series of exchanges and single-temperature Monte Carlo moves is depicted in Figure 2.3.1.

If we assume that system is having Gaussian energy distributions, average acceptance rate  $\langle A \rangle$  can be defined as:

$$A = \text{erfc} \left[ \left( \frac{1}{2} C_v \right)^{1/2} \frac{1 - \beta_j / \beta_i}{(1 + (\beta_j / \beta_i)^2)^{1/2}} \right] \quad (2.21)$$

where:

$C_v$  is the heat capacity having a constant volume in a temperature range from  $\beta_i$  to  $\beta_j$

In the equation above the average acceptance rate varies based on the probability that replica having a higher temperature, arrives to the phase space region relevant to replicas at the lower temperatures. The above formulation of the average acceptance rate plays the important role in decision making process regarding the choice of the replica temperatures in the Parallel Tempering simulation.

### 2.3.2 Theory of Replica Exchange Molecular Dynamics

In contrast to the Monte Carlo RE simulations, where only positions of the particles are taken into account, REMD simulations must also consider the momenta of all the particles defining

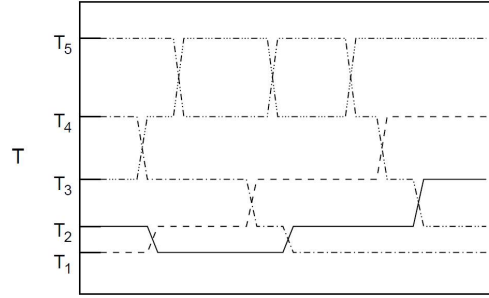


Figure 2.1: Schematic representation of exchanges between neighboring replicas at different temperatures [12]

the system of interest. According to the REMD method devised by the Sugita and moto the momenta of the replica  $i$  after the successful exchange can be calculated by:

$$p^{(i)'} = \sqrt{\frac{T_{new}}{T_{old}}} p^{(i)} \quad (2.22)$$

where:

$p^{(i)}$  is the old momenta for replica  $i$

$T_{old}$  is replica temperature before the exchange

$T_{new}$  is replica temperature after the exchange

The above equation ensures that the average kinetic energy can be calculated as:  $\frac{2}{3}Nk_B T$ . The probability that the exchange will be accepted is the same as for the Monte Carlo RE method and can be calculated using equation (1.2).

### 2.3.3 Optimal Choice of Temperatures

In order to maximize sampling quality and to minimize required computational effort, it is vital to correctly choose the temperatures for the replicas as well as the number of replicas involved in the REMD simulation. The choice of temperatures is motivated by the need to avoid the situation when some of the replicas are "trapped" in local energy minima. At the same time, it is also important to have enough replicas, for the exchanges to be performed between all "neighboring" replicas. From the equation (1.2) and Figure 2.2 it is obvious that in order for exchanges to be accepted, energy histograms of adjacent replicas must have some overlapping parts. It was demonstrated that using a geometric progression for temperatures, so that  $\frac{T_i}{T_j} = \text{constant}$  for the systems having a constant volume heat capacity  $C_v$  for the whole temperature range, allows to achieve equal exchange acceptance probability for all participating

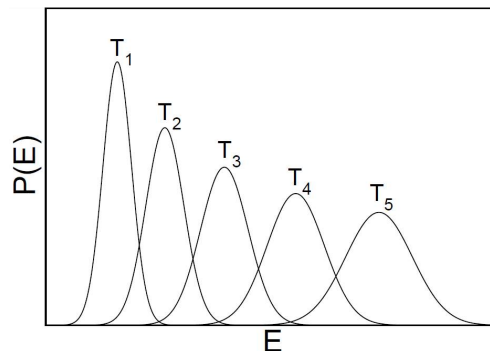


Figure 2.2: Energy histograms for a system at five different temperatures [12]

replicas [12]. Various studies [13] [14] showed that exchange acceptance probability around 20% results in best possible performance of the RE simulation.

A great care should be taken then analyzing the results of the REMD simulations. It is important always to remember that REMD simulations simply allow us to perform a variant of phase space sampling, meaning that we cannot make any assumptions about the dynamics of the analyzed system, since performed exchanges are not physical processes.

## 2.4 Quantum Mechanics/Molecular Mechanics

In hybrid quantum mechanics / molecular mechanics (QM/MM) simulations, the system is divided into two regions: the quantum mechanics region, in which the chemical process takes place, is simulated using quantum chemistry theory, the molecular mechanics region, constitutes the remainder of the system and is described by a molecular mechanics force field. QM/MM methods was originally introduced by Warshel and Levitt [? ]. QM/MM enables the study of the chemical reactivity in large systems, such as enzymes [? ]. QM/MM method is depicted in Figure 2.3.

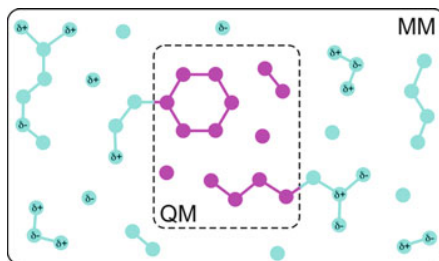


Figure 2.3: Illustration of the QM/MM method. A region, in which a chemical reaction occurs (cannot be described with a force field), is described by quantum mechanical theory. The remainder of the system is modelled using molecular mechanics [? ].



In molecular mechanics we describe the potential energy of the system as:

$$U_{MM} = \sum_i^{N_{bonds}} U_i^{bond} + \sum_j^{N_{angles}} U_j + \sum_l^{N_{torsions}} U_l^{torsion} + \sum_i^{N_{MM}} \sum_{j>i}^{N_{MM}} U_{ij}^{coul} + \sum_i^{N_{MM}} \sum_{j>i}^{N_{MM}} U_{ij}^{LJ} \quad (2.23)$$

where:

$N_{MM}$  - the number of atoms in the system

$U^{bond}$  - bonds (modelled using harmonic functions)

$U^{angle}$  - angles (modelled using harmonic functions)

$U^{torsion}$  - torsions (modelled using periodic functions)

$U_{ij}^{coul}$  - the pairwise electrostatic interaction between atoms with a partial charge ( $Q_i$ )

$U_{ij}^{LJ}$  - Lennard-Jones potential

We calculate  $U_{ij}^{coul}$  using Coulomb's law:

$$U_{ij}^{coul} = \frac{e^2 Q_i Q_j}{4\pi\epsilon_0 R_{ij}} \quad (2.24)$$

where:

$R_{ij}$  - the interatomic distance

$e$  - the unit charge

$\epsilon_0$  - the dielectric constant

The Lennard-Jones potential is given by:

$$U_{ij}^{LJ} = \left( \frac{C_{12}^{ij}}{R_{ij}} \right)^{12} - \left( \frac{C_6^{ij}}{R_{ij}} \right)^6 \quad (2.25)$$

where:

$C_{12}^{ij}$  - repulsion parameter (depends on the atomtypes of the atoms  $i$  and  $j$ )

$C_6^{ij}$  - attraction parameter (depends on the atomtypes of the atoms  $i$  and  $j$ )

In molecular mechanics electrons are ignored. Influence of electrons is modelled by empirical parameters. As a consequence, processes that involve electronic rearrangements, such as chemical reactions, cannot be described in molecular mechanics. To describe these processes are used quantum mechanics, where the electronic degrees of freedom can be defined. Evaluation of the electronic structure, is very computationally intensive and as a result the size of the system of interest often is restricted in size.

Many biochemical systems can't be easily described at a single level of theory due to their

large size. In addition, molecular mechanics are lacking in flexibility when used to model processes in which chemical bonds are broken or formed [? ].

The QM/MM method stems from the nature of the most chemical reactions. Often it is possible to make a clear distinction between a reaction region, where atoms that are directly involved in the reaction and a remainder of the system, where direct participation of the atoms in the chemical reaction is not observed. For most enzymes, the catalytic process is restricted to an active part, often located inside the protein. The rest of the system provides an electrostatic background that is not necessarily facilitating a reaction.

Potential energy in QM/MM is divided into three interaction types: interactions between atoms in the QM region, interactions between atoms in the MM region and interactions between QM and MM atoms. Atom interactions in QM and MM regions are described by the corresponding theories. Interactions between QM and MM atoms can't be easily described. To address this issue a number of approaches were proposed, which can be divided into two categories: subtractive and additive coupling schemes.

## 2.5 Asynchronous Replica Exchange

We now discuss synchronization scenarios for Replica Exchange simulations from software design perspective. First, it is essential to justify the importance of this discussion and to motivate the need for asynchronous RE (Figure 2.4 (b)) from scientific perspective.

RE algorithms have historically been synchronous, viz., there is a global barrier between the simulation and exchange phases (Figure 2.4 (a)). Asynchronous RE (Figure 2.4 (b)) refers to the scenario when replicas can be in different phases. For example, a subset of replicas might be exchanging while some replicas might still be in simulation phase. In other words, the global synchronization of regular RE is relaxed. Asynchronous RE has the following scientific advantages:

**Facilitates adaptive sampling.** There are cases, where some replicas have already produced sufficient info and are no longer needed. For example, replicas simulating configuration space with very low probability may not need high accuracy hence only relatively small amount of sampling is required. Consequently these replicas should be terminated and their computational resource should be released. On the other hand, in the midst of simulations, new replicas may need to be created to cover the regions where more sampling is necessary. Obviously asynchronous algorithms are needed in such cases.

**Enables integration of heterogeneous simulations.** Nowadays multi-scale molecular

simulations may consist of very different levels of theories hence different replicas may have significant differences in performance. For example, quantum mechanics calculations usually are slower than classical molecular dynamics simulations. As a result, it is desired to have asynchronous RE algorithms to handle simulations with large mismatch in performance.

**Handles fault-tolerance.** Large-scale RE simulations, are more receptive to both hardware and software failures, which result in failures of individual replicas. Hence it is necessary to recover from such failures and continue simulation. Due to the nature of asynchronous algorithms, recovery time is significantly reduced compared to a synchronous RE, where in case of a failure all other replicas must wait at the barrier for a restarted replica.

**Manages load-balance with fluctuation of available resources.** Multi-dimensional RE simulations may require very large numbers of replicas, which could be larger than the available number of CPUs. In addition, both the number of running replicas and availability of a resource could change during simulation. Traditional synchronous algorithms are not capable to handle such cases. Asynchronous algorithms are needed to execute replicas at different time so that simulations of all replicas can be performed.

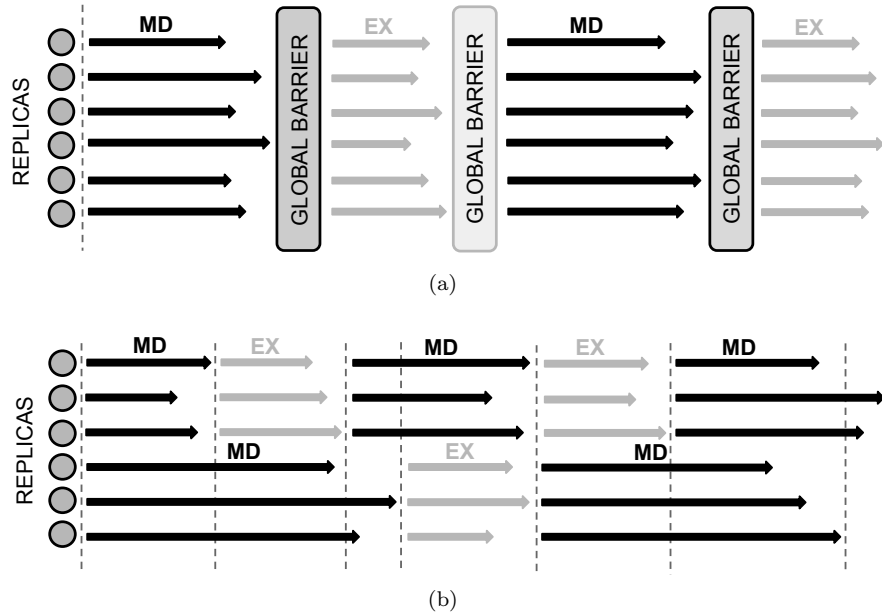


Figure 2.4: Schematic representation of Replica Exchange Patterns: (a) Synchronous (b) Asynchronous. x-axis represents time. Gray squares represent replicas, blue arrows MD phase propagation and green arrows exchange phase propagation. For both phases (MD and exchange), in synchronous pattern exists a global synchronization barrier. In this figure, for synchronous pattern, both MD and exchange are propagated concurrently but this is not a requirement for this pattern. In asynchronous pattern there is no barrier - MD and exchange can be propagated concurrently, meaning while some replicas run MD other replicas might be running exchange.

## 2.6 Multi-dimensional REMD

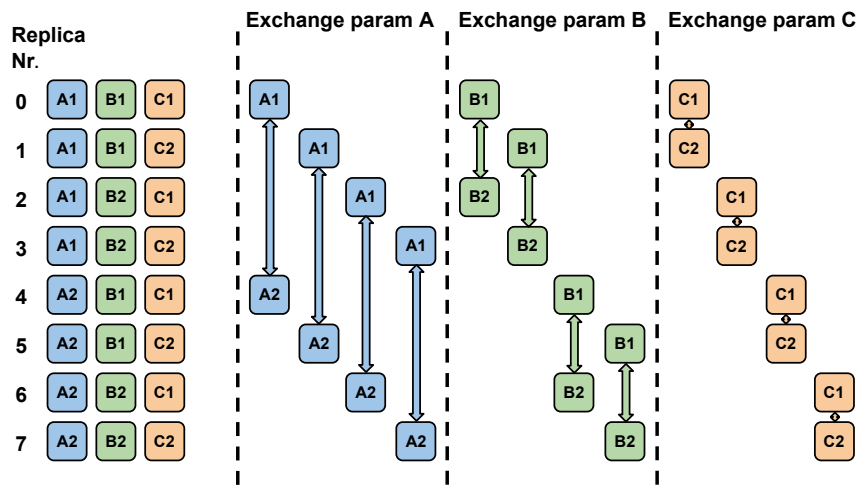


Figure 2.5: Schematic representation of the parameter exchange schema for the three-dimensional REMD. A, B and C are artificial parameters, which are exchanged between replicas belonging to the same group. For the exchange in any given dimension replicas are grouped based on their parameters in other two dimensions. To be grouped together in dimension 1, parameters of replicas in dimensions 2 and 3 must be equal. In this diagram, group sizes in all dimensions are equal to two. Generally, this is not a requirement - group sizes can exceed this number.

In Figure 2.5 is depicted a parameter exchange schema for a three-dimensional REMD. For illustration purposes we use artificial parameters A, B and C, which represent parameters in three respective dimensions. Although not shown in Figure 2.5 before an exchange of each parameter is performed an MD phase. In multi-dimensional REMD simulation parameters are exchanged sequentially - first is performed an exchange in first dimension, then in second and so on. In Figure 2.5 the total number of replicas is eight. While this simplifies the schema, it also limits the group sizes in all dimensions to two replicas. In each dimension, replicas are grouped based on the values of their parameters in other two dimensions. For example, replicas 0 and 4 are in the same group in dimension one (parameter A), since their parameters B and C are equal. It is important to note that group contents are changing dynamically - exchange of replica parameter in any given dimension determines its group partners in other dimensions.

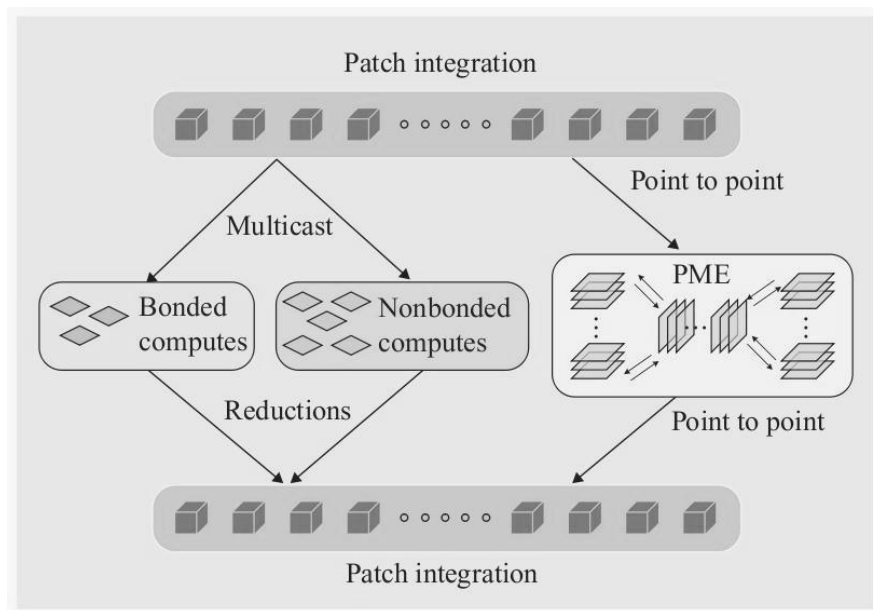


Figure 2.6: Schematic representation of NAMD parallelization mechanism [15]

## 2.7 Molecular Simulation Software Packages with Integrated REMD Capability

### 2.7.1 Nanoscale Molecular Dynamics - NAMD

NAMD [2] is a parallel molecular dynamics application which is aimed at simulations of biomolecular systems. NAMD can be used on various systems, starting with regular desktops and ending with the most powerful HPC systems available today. Often problem size of the biomolecular simulations is fixed and systems are analyzed by performing a large number of iterations. This means that MD applications must be highly scalable. A parallelization strategy used in NAMD is a hybrid of force decomposition and spatial decomposition. In addition to that, NAMD uses dynamic load-balancing capabilities of the Charm++ parallel programming system. [15]

#### **NAMD parallelization strategy:**

Parallelization in NAMD uses a hybrid strategy, consisting of spatial decomposition and force decomposition. This is complemented by the dynamic load-balancing framework of the Charm++ system. In Molecular Dynamics, calculation of the non-bonded forces between all pairs of atoms is the most computationally demanding. The algorithm for this calculation has a time complexity of  $O(n^2)$ . In order to reduce time complexity of this algorithm to  $O(n \log n)$ , the terms cutoff radius  $r_c$ , separation of computation of short-range forces and separation of

computation of long-range forces were introduced [15]. For the atoms within the cutoff radius  $r_c$  non-bonded forces are calculated on per atom basis. For the atoms outside the  $r_c$ , long-range forces are calculated using particle-mesh Ewald algorithm, which has a  $O(n \log n)$  time complexity. Decomposition of MD computation in this way, results in calculation of non-bonded forces for atoms within the  $r_c$  being responsible for 90% of total computational effort.

A well known problem, arising from parallelising MD simulations using as a base sequential codes, is poor scalability. Scalability is often measured using isoefficiency, which is defined as a rate of change of problem size required to maintain parallel efficiency of the increasingly parallel system. Isoefficiency is defined by:

$$W = \frac{1}{t_c} \left( \frac{E}{1 - E} \right) T_o \quad (2.26)$$

or, if  $K = E/(t_c(1 - E))$  is constant depending on efficiency:

$$W = KT_o \quad (2.27)$$

where:

$W$  - is problem size

$t_c$  - is cost of executing each operation

$E$  - is parallel efficiency;  $E = \frac{S}{p}$  where  $p$  is number of processors and  $S$  is speedup;  $S = \frac{T_1}{T_P}$  where  $T_1$  is sequential runtime and  $T_P$  is total parallel runtime

$T_o$  - is total overhead

Small rate of change of problem size  $W$  means that in order to efficiently utilize increasing number of processors, relatively small increments in problem size are required. This means that parallel program is highly scalable. On the other hand, large rate of change of  $W$ , indicates that parallel program scales poorly.

For MD simulations scalability is often limited by the rate of change of communication-to-computation ratio, which increases too rapidly while increasing the number of processors. This limitation leads to "large" isoefficiency function, meaning that weak scaling is poor for the particular code.

In order to avoid issues specified above, NAMD uses a hybrid parallelization strategy, which is a combination of spatial decomposition and force decomposition. This strategy is aimed to allow increase of parallelism without proportional increase of communication cost. This strategy involves dividing a simulation space into *patches* - cubic boxes, size of which is calculated based on the cutoff radius  $r_c$ . The size of a *patch* is determined based on parameter  $B$ . The length of a *patch* in each dimension is  $b = \frac{B}{k}$  and  $B = r_c + r_H + m$ , where  $r_H$  is the maximum length

of a bond to a hydrogen atom times two,  $m$  is the margin equal double distance that atoms may move without being required to migrate between the patches and  $k$  is a constant [15]. The value of constant  $k$  is from the set  $\{1, 2, 3\}$ . A *one-way decomposition* can be observed when  $k = 1$ , which typically results in having from 400 to 700 atoms per *patch*. With  $k = 2$  number of atoms per *patch* decreases to approximately 50 atoms.

With NAMD 2.0, to the spatial decomposition described above was added a force decomposition, forming a hybrid parallelization. NAMD force decomposition can be described as follows. A *force-computation object* or *compute object* is initialized for each pair of interacting *patches*. For example, if  $k = 1$  the number of *compute objects* is fourteen time greater than the number of *patches*. *Compute objects* are mapped to processors, which in turn are managed by the dynamic load balancer of *Charm++*. This strategy also exploits Newton’s third law in order to avoid duplicate computation of forces [15]. A schematic representation of this hybrid parallelization strategy utilizing *patches* and *compute objects* can be found in Figure 2.6.

NAMD is based on *Charm++* - a parallel object-oriented programming system written in C++. *Charm++* is designed to enable decomposition of computational kernels of the program into cooperating objects called *chares*. *Chares* communicate with each other using asynchronous messages. The communication model of these messages is single sided - a corresponding method is invoked on a compute object only then a message is received and no resources are spent on waiting for incoming messages (e.g. posting a receive call). This programming model facilitates latency hiding, while demonstrating good resiliency to system noise. A processor virtualization feature of *Charm++* allows the code to utilize a required number of compute objects in order to meet its requirements. Typically several objects are assigned to a single processor and execution of objects on processors is managed by the *Charm++* scheduler. Scheduler performs a variety of operations, including getting messages, finding destination *chare* of each message, passing messages to appropriate *chares* and so on. *Charm++* can be implemented on top of MPI without using its functionality, which makes NAMD a highly portable program.

### 2.7.2 The Amber Molecular Dynamics Package

Computer MD simulations enable investigation of the dynamics and structure of proteins. Some examples are enzyme reaction mechanisms, ligand binding and protein refolding. Amber is one of the most popular MD simulations software packages. Amber is a collection of the various programs working together to setup, run and analyze MD simulations for proteins, carbohydrates and nucleic acids. In addition Amber also is a name of a set of classical molecular mechanics

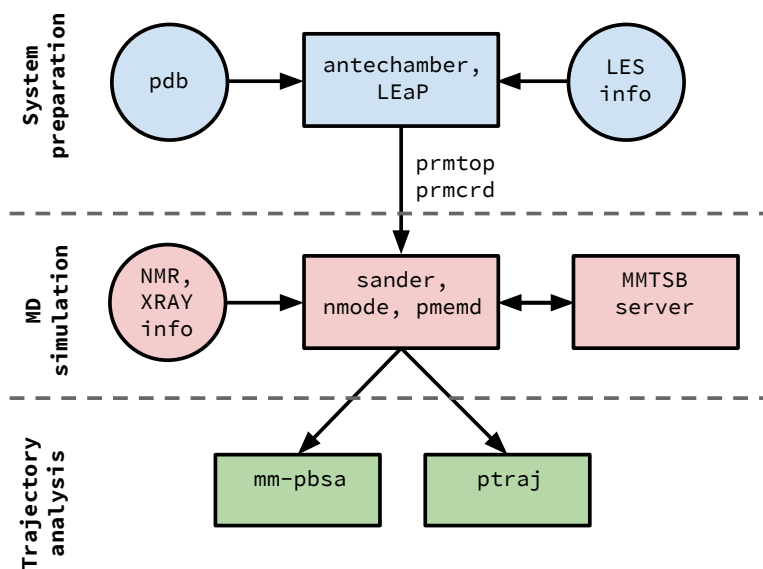


Figure 2.7: Information flow in the Amber program suite

force fields, developed for the simulation of biomolecules. Interestingly, some other MD software packages have implemented the Amber force fields and Amber itself can be used with other force fields.

Amber is a result of a joint effort of the more than 40 researchers, who are working on advancing MD methodology. MD simulation part of Amber package consists of the four tightly coupled programs: `sander`, `sander.MPI`, `pmemd` and `pmemd.cuda`. Popularity of the Amber force fields, and their adoption by other MD software packages motivated the decision to separate Amber’s setup and analysis tools into a separate package named AmberTools.

In Figure 2.7 is provided a schematic representation of the information flow in Amber. A typical simulation with Amber can be divided into three steps: system setup, MD simulation and trajectory analysis. Tools at the top layer of the Figure 2.7 are responsible for the system preparation. Middle layer of the figure represents MD simulation tools. At the bottom layer of the Figure 2.7 are depicted trajectory analysis tools. Naturally, collaborative nature of the development, resulted in separation of Amber into various programs. This approach enabled the usage of different programming languages and software engineering practices by developers of these programs. For example, LEaP is written in C using X-window libraries, MD simulation programs are written in Fortran 90, but `mm-pbsa` is written in Perl. Historically, system preparation and analysis programs were considered less computationally intensive in comparison with simulation programs. As a result, most of the performance optimization effort went



into MD simulation programs. In contrast with MD programs, which run on HPC clusters, system preparation and analysis programs often are executed on a users workstation. Amber’s development approach enables integration of other MD software into Amber’s software stack. For example, Amber tools and force fields can be used by NAMD. To achieve this, NAMD must parse and interpret information provided by `.prmtop` files. In addition, there is a number of software packages, which are aimed at improving Amber’s preparation interface. Some of these extensions use portion of LeAP’s code, others are entirely written from scratch.

As shown in Figure 2.7, in Amber there are four system preparation programs. Out of these four programs, major programs are LEaP and antechamber. The former is responsible for construction of biopolymers from the component residues, preparation of lists of force field terms and solvation of the system. The latter is responsible for creation of the force fields for residues. System preparation phase generates two files: parameter-topology files (`.prmtop` format) and coordinate file (`.prmcrcd` format). As the name suggests, the latter contains coordinates of all atoms in the system. The former contains information required to compute forces and energies, such as: mass of the atom, atom name, lists of bonds, force field parameters, angles, and dihedrals. Despite being fairly basic, Graphical User Interface (GUI) of LEaP not only provides a visual representation of the PDB files, but also allows to perform interactive altering of the structure. In addition to GUI, LEaP also provides a text mode, which is the main usage mode of this program.

Central molecular dynamics program in Amber is `sander`. This program is written in Fortran 90. `sander` reads input parameters as a label-value pairs. There are more than 150 different input parameters in `sander`, but in most simulations around 1/5 of these parameters is actually used.

A parallel version of `sander` is called `sander.MPI`. In `sander.MPI` to each process is assigned a certain number of atoms, while all atoms are organized in a single data structure. Coordinates of all atoms are available to all active processes. During the simulation, for each simulation step processes calculate potential energy and corresponding gradients. Force vector is calculated by gathering individually computed data by all processes, which results in each process obtaining the full force vector for its assigned atoms. Next, processes perform a molecular dynamics simulation step and communicate updated positions of their assigned atoms to all the processes. This enables multiple approaches for collective calculation of force fields by active processes.

Frequent all-to-all communication hinders scalability of `sander.MPI`. In addition, system size has a significant effect on the size of the data structures used for the communication and

on the amount of communicated data itself. Consequently, explicit solvent molecular dynamics simulations with `sander.MPI` do not scale linearly when number of nodes is greater than 12. Due to a smaller number of force fields and coordinates, implicit solvent molecular dynamics simulations demonstrate a much better scalability.

To address performance limitations of `sander` was developed `pmemd`. In this code were made optimizations for both parallel and serial performance. While `pmemd` supports only the most popular simulation types, it provides significant performance improvements in comparison with `sander`.

Amber’s analysis program is called `ptraj`. There is a number of challenges associated with MD trajectory analysis. First, is management of trajectory files. Files are generated at different times and the number of files can be quite large. In addition, the size of the trajectory files can be very large. Next, multiple types of analysis may be required as the simulation is propagated. The `ptraj` is capable to process Amber and CHARMM trajectory file formats (`.prmtop` and `.psf` respectively). The `ptraj` also is capable of composing trajectories from partial trajectories and removing unnecessary parts of trajectories (solvent) if needed. The `ptraj` provides capability for users to add new analysis commands. The `ptraj` is a cluster of programs, which perform analysis such as energy estimation, entropies estimation, etc.

## 2.8 REMD Software Frameworks

In this section, we focus on frameworks designed to implement RE algorithm outside of the MD engine; we defer a discussion of REMD simulations using molecular simulation software packages with integrated RE capability till later. We start with CHARMM based implementation for 2D REMD. Then we introduce Multiple Copy Algorithm (MCA) implementation with NAMD engine and finally we discuss implementations of asynchronous Replica Exchange.

### 2.8.1 CHARMM

Ref. [16] presents an implementation of a 2D US/H-REMD method, implemented in `REPDSTR` module of the CHARMM [17]. `REPDSTR` uses an MPI level parallel/parallel mode where to each replica are assigned multiple MPI processes and dedicated I/O routines. Exchanges of parameters between neighboring replicas in first dimension are implemented using odd-even rule and in second dimension using even-odd rule. To improve sampling efficiency exchange attempts are performed alternatively along the two dimensions.

Implementation was tested on IBM Blue Gene/P supercomputer using the binding of calcium ions to the small protein Calbindin  $D_{9k}$ . Obtained results show that 2D US/H-REMD significantly improves the configurational sampling for biological potential of mean force (PMF) calculations and as a result facilitates convergence of the simulation.

Authors presented strong scaling performance of 2D US/H-REMD, involving 4096 replicas and utilizing up to 131072 CPUs with nearly linear scaling.

### 2.8.2 MCA implementation with NAMD

A Charm++ based implementation designed to run MCA was presented in [18]. It is tightly bound to the NAMD simulation engine. Charm++ is used to run concurrently multiple NAMD instances, which are exchanging messages via a point-to-point communication functions of Tcl scripting interface. Tcl scripting enables users to implement REMD algorithms without modifying the source code.

Authors demonstrated strong scaling behavior of the swarms-of-trajectories string method implementation using the full-length c-Src kinase system utilizing up to 524288 cores on Blue Gene/Q supercomputer. Results of temperature exchange REMD simulations with peptide acetyl-(AAQAA)<sub>3</sub>-amide [19] in TIP3 solvent on Blue Gene/Q (utilizing up to 32768 cores) were presented. Implementation of two-dimensional Hamiltonian Replica Exchange with Umbrella Sampling (US/H-REMD) on irregular-shaped distribution of umbrella windows was discussed.

### 2.8.3 ASyncRE package

Ref. [20, 21] presented ASyncRE package, developed to perform large-scale asynchronous REMD simulations on HPC systems.

ASyncRE has an emphasis on asynchronous RE. Package supports Amber [7] and IMPACT [22] MD engines. It implements two REMD algorithms, namely multi-dimensional RE umbrella sampling with Amber and BEDAM  $\lambda$  RE alchemical binding free energy calculations with the IMPACT. ASyncRE uses a similar runtime system as RepEx, is capable of launching more replicas than there are CPU cores allocated and is fault tolerant: failure of a single (or multiple) replicas does not result in failure of a whole simulation. Upon the user request failed replicas can be ignored or relaunched.

In ASyncRRE duration of the simulation phase is defined as a real time interval. This allows to perform synchronous RE simulations with ASyncRE, by specifying a sufficiently large duration for the MD simulation phase and allocating enough CPU cores to run all replicas

concurrently. The major drawback of running synchronous RE simulations with ASyncRE are substantially increased simulation’s Total Time to Completion (TTC) and significant under utilization of allocated CPU cores on a remote system.

#### 2.8.4 Asynchronous Replica Exchange Package for Volunteer Computing Grids and HPC clusters

Ref. [23] introduced another REMD package targeted at asynchronous RE, optimized for volunteer computing resources. The package can be used on HPC clusters as well. It is customized for IMPACT and supports both 1D and 2D REMD simulations.

Distinctive features are fault tolerance, the ability to use a dynamic pool of resources and to use fewer CPU cores than replicas. Input files are generated on a user’s workstation and exchange phase is performed on coordination server, meaning that output data must be moved from target resource to coordination server. Implementation specifics enforce the length of the MD simulation phase to be greater than 1ps. Implementation was evaluated using statistical inefficiency analysis [24] and divergence of the binding energy distribution from a target distribution, using the Kullback-Leibler divergence [25] for both 1D REMD and 2D REMD BEDAM [26] simulations using b-cyclodextrin-heptanoate model and using up to 240 replicas.

#### 2.8.5 Summary

As seen, there are multiple existing packages designed to perform REMD simulations. A significant number of them however, support a single MD engine, and their design makes it difficult to substitute simulation engines. The tight binding of RE methods to a particular engine raises a barrier for the development of new RE algorithms.

Historically, tight integration has prevailed due to the perception that performance trumps all other features. There are emerging examples of important biomolecular problems however, that involve multi-state equilibria, and for which the interpretation of experiments requires scanning control variables such as temperature, ionic conditions, and pH in addition to geometrical or Hamiltonian order parameters[27]. These applications have the added challenge that sampling along the space of the order parameters needs to be statistically converged at all points. Here, the REMD method offers the added advantage that equilibrium between simulations is enhanced through the exchanges. An illustrative example is the "problem space" associated with biocatalysis whereby conformational equilibria, metal ion binding and protonation events lead to an active state that can catalyze the chemical steps of the reaction [28]. Thus, these

applications require not only the elucidation of the free energy landscape of the chemical reaction itself [29, 30], but also the characterization of the probability of finding the system in the catalytically active state as a function of system variables [31].

To address these novel applications and scenarios, a flexible and efficient multi-dimensional REMD framework is required, that can be used for both system control variables and generalized coordinates. Currently, there is no REMD framework capable of providing the necessary flexibility in composing the range of RE methods with MD engines as needed, while providing adequate performance.

## 2.9 Pilot Systems

Traditionally many HPC systems are designed to support workloads consisting of a single parallel executable. At the same time, there are numerous use-cases in various scientific domains, which can take advantage of the capability to run workloads of multiple heterogeneous tasks. Often these tasks have complex dependencies, vary in computational requirements and are created on demand. To execute these workloads, is required an API, which enables fine-grained management of tasks and control over allocated computational resources. Currently HPC systems are lacking such interface. Pilot systems enable execution of complex, multi-task workloads by decoupling of workload specification, resource selection, and task execution via job placeholders. Pilot systems provide an interface to HPC systems, which enables a flexible usage of the available computational resources, while complying to usage policies of these systems. To access control over computational resources, pilot system submits job placeholders (i.e., pilots) to the schedulers of the HPC resources. First, pilots are waiting in schedulers queue until there are enough CPUs available. Then, pilots perform setup procedure (i.e. bootstrap) and are ready to execute tasks. Tasks are executed within the time frame requested by the user.

There are many scientific workloads consisting of large ensembles of tasks (both single and multi-core) which have computational requirements exceeding the size of the allocatable resources. Execution of such workloads on HPC clusters, using conventional techniques is cumbersome or even impossible.

From a user perspective, pilot systems provide two clear advantages. First, pilot systems allow to reduce the total time to completion (TTC) for ensemble of jobs. Two major components of the TTC are queue waiting time and total execution time of individual jobs. Second, pilot systems provide means to define complex workloads at application level and manage their execution on HPC systems.

Historically most of the pilot systems were developed for a specific user communities, resources or workloads. The first pilot system was developed as early as 1996, when AppLeS [?] system introduced features such as application-level scheduling and a concept of a resource placeholder. Later, more pilot systems, targeting various communities and resources emerged. Some of the well known pilot systems are: BOINC [?], DIANE [32], Falkon [33], DIRAC [34] and BigJob [?]. Two notable examples of pilot systems are HTCondor [?] and Glidein [?]. These systems introduced concurrent execution of workloads on multiple resources and currently are amongst the most widely used pilot systems. Another notable example is ATLAS PanDA [?], which is used to run millions of jobs a week on a Worldwide LHC Computing Grid (WLCG). An example of a workload specific pilot system is CRAM [?]. CRAM is designed to execute ensembles of MPI tasks on HPC clusters and was developed specifically for the Sequoia supercomputer at Lawrence Livermore National Laboratory (LLNL). Another examples is Pegasus-MPI-Cluster (PMC) [?], which is an MPI-based Master/Worker framework that can be used in combination with Pegasus workflow management system [?]. It runs large-scale workflows of small tasks (limited to a single node) on HPC resources. An example of a pilot system for HPC resources, which provides an API is Falcon [?]. Application developers can use Falcon’s API to develop distributed applications for execution of their workloads. One of the Falcon’s limitations is focus on a single-core tasks.

Features of pilot systems make them a good workload execution mechanism for applications designed to perform REMD simulations. In particular, decoupling of the workload specification and task execution. This enables application developers to significantly increase fault tolerance of the respective applications.

Despite the fact that the notion of the pilot system is fairly established, the industry standard model for pilot systems doesn’t exist. Designs of the pilot systems often have significant differences. This can be explained by the fact that these systems often targeting specific resources, workload and user communities. As the result, portability and extensibility of these systems is limited. Additionally, many pilot systems introduce new definitions and concepts, making it almost impossible to compare them in a meaningful way. To address this issue, Luckow et al. proposed a *P\* Model of Pilot Abstractions*, aimed to be a unified standard model suitable for various target architectures and frameworks [35]. The main goal of P\* Model is to provide a convenient means to qualitatively compare and analyze various pilot systems.

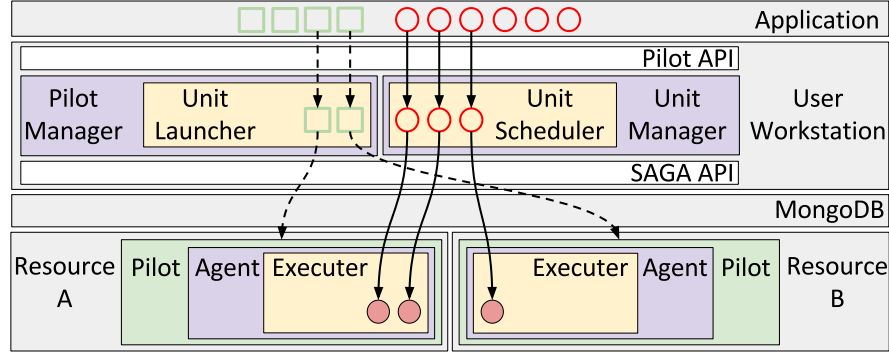


Figure 2.8: RP overview. An application uses the Pilot API to describe pilots (green squares) and units (red circles). The PilotManager instantiates (dash arrow) pilots, the Unit-Manager instantiates (solid arrow) units. Both managers are executed on the user workstation. Pilots are launched (dashed arrows) on resources A and B via SAGA API, an Agent is bootstrapped for each pilot, units are scheduled (solid arrow) to the Agents via MongoDB and executed by the Agents Executer. Boxes color coding: gray for entities external to RP, white for APIs, purple for RPs modules, green for pilots, yellow for modules components.

## 2.10 RADICAL-Pilot

RADICAL-Pilot (RP) is a portable, modular and extensible pilot system written in Python programming language. RP is capable of spawning more than 100 tasks/second and the steady-state execution of up to 8,000 concurrent tasks. RP can be used stand-alone, as well as integrated with other application-level tools as a runtime system. A distinct feature of RP is its API - "Pilot API" [? ], which can be used by application developers to orchestrate execution of their workloads on HPC systems. Pilot API is designed to enable users to describe pilos and workloads (comprised of multiple tasks), which are then passed to the RPs runtime system. RP utilizes a Simple API for Grid and Distributed Applications (RADICAL-SAGA [? ]) as an interface to the HPC systems. Unlike some other pilot systems, RP does not provide workload management capabilities. RP supports execution of ensembles consisting of both MPI (including multi-node tasks) and non-MPI tasks on various HPC resources.

In RP, pilots are represented as collections of computational resources, which are independent from the architecture of the target resource. Workloads are represented as a collections of units, which are executed by a pilot. Both pilots and units have a state model associated with them. States of the pilots are managed by the PilotManager, but states of the units by Unit Manager and Agent (Figure 2.8). To launch pilots on HPC resources, PilotManager is using SAGA API. SAGA is providing adaptors for various scheduling systems and types of the resources, which enable management of jobs and files. As a communication channel between UnitManager and Agents RP uses a MongoDB database. UnitManager is responsible for scheduling units for execution on available pilot instances. First, pilot is submitted to the queue

of a resource scheduler. When pilot becomes active, Agent gets bootstrapped on allocated CPU cores. Then Agent starts pulling units from the MongoDB database and executes them on CPU cores allocated by the pilot.

RP is a distributed system, with PilotManager and UnitManager running on a user workstation and Agent running on a remote resource. Launcher component of the PilotManager specifies the number, properties and placement of the Agent components (Stager, Scheduler, and Executer) on a Pilot. To achieve this, Launcher is using resource configuration files, which are defined for various resource types. Placement of the Agent components depends on the resource type. On HPC clusters, Agent components can be placed on the cluster's MOM nodes, login nodes or compute nodes. Agent components use ZeroMQ for communication, which facilitates transitions of the units. After Agent becomes active, its Scheduler queries the resource manager for the number of cores allocated by the pilot and their topology on a cluster. Scheduler is capable to get resource info from the following resource managers: Sun Grid Engine (SGE), PBS Professional, Simple Linux Utility for Resource Management (SLURM), TORQUE, Cray CCM, LSF and LoadLeveler. Currently RP supports two scheduling algorithms: "Torus" for CPUs comprising an n-dimensional torus (such as on IBM BG/Q) and "Continuous" for CPUs connected continuously. Once Scheduler obtains resource information, it passes the units to Executer components, which launch units using launching method, specified in the resource configuration file. RP supports the following launching methods: IBRUN, ORTE, APRUN, MPIRUN, MPIEXEC, CCMRUN, RUNJOB, DPLACE, RSH, SSH, POE, and FORK. Executer uses one of the two spawning mechanisms for unit execution: Popen (Python based) and Shell (based on `/bin/sh`). Executer monitors unit execution, collects exit codes and reports to Scheduler once units finish executing.



## Chapter 3

### Requirements

In this sub-section, we motivate and define requirements of a REMD simulations software. We describe three types of requirements: functional, performance (scalability) and usability. We identified the following functional requirements:

**Generality** is a requirement to maximize a range of replica-exchange methodologies as well as MD engines. A general purpose framework should support: (i) different types of exchange parameters, (ii) multiple exchange parameters in a single REMD simulation, and (iii) multiple MD engines. A corollary of this requirement is the decoupling of advances in replica-exchange methodology to MD engines, and thus the potential for broader (greater number of REMD applications) and deeper impact (enable new research opportunities).

**Execution flexibility** arises from the need to decouple the number of CPU cores from the number of replicas. Alternatively, the ability to set-up a REMD simulation with a desired number of replicas, independent of the number of CPU cores available at a given instance of time. For reasons ranging from a queue waiting time to limitations in the number of allocatable CPU cores on a given cluster, it should be possible to use as many or as few CCPU cores as needed, irrespective of the number of replicas. The same principle also applies to individual replicas: support for both single-core and multi-core replicas should be provided. Currently, **all** REMD frameworks require at least as many CPU cores as replicas; furthermore, the number of replicas that are actively simulated is fixed and statically determined.

**Synchronization.** To enable a wider range of REMD simulations support for asynchronous RE is required without loss of generality or execution flexibility.

**Interoperability.** Most REMD simulations are executed on supercomputers which vary in scheduling systems, middleware and software environment. To support community production grade science, a REMD framework should work on multiple high-end machines as well as small HPC clusters, while retaining functionality and performance.

The above functional requirements have to be balanced with the following performance requirements:

**Scalability with the number of replicas.** To obtain high sampling quality, REMD simulations should support the ability to run a large number of replicas. Furthermore, given that the number of replicas needed for a REMD simulation scales as  $\approx N^d$ , where  $d$  is the dimensionality (of exchange), the need to support a large number of replicas is greater when applied to multi-dimensional simulations. Achieving good scalability for REMD frameworks is a challenging task, especially when preserving the four functional requirements outlined above.

**Scalability with the number of CPU cores.** Whereas the primary performance metric is the scalable execution of a large number of replicas, it is often the case that each replica is multi-node (in Ref. [36], each replica was 768 cores); multi-node replicas are important to simulate large physical systems. Any framework should provide scalability in the number of replicas simulated and the number of CPU cores utilized.

**Usability.** Relative to the simulation phase, the exchange phase is significantly more complex. Thus, not only should a framework for REMD separate the logic of the exchange mechanisms from the simulation mechanisms, it should not expose the complexity of exchange mechanism, should be automated as much as possible and must be fully specified by configuration files. Definition of configuration files should be intuitive and should include a minimal set of parameters.

## Chapter 4

### Design

To satisfy the requirements outlined in the previous sub-section, we discuss the three concepts underpinning the unique design of RepEx:

- **Replica Exchange Pattern:** explicit support for synchronization patterns between simulation and exchange phases.
- **Pilot-Job system:** a multi-stage mechanism for workload execution via the use of an initial placeholder job (the “pilot”) and thus dynamically allocating computational resources for replicas.
- **Flexible Execution Mode:** The ability to execute different patterns and number of replicas independent of the underlying resources available, i.e., flexible spatial and temporal mapping of workload (tasks) to the allocated CPUs.

#### 4.1 Replica Exchange patterns

The RepEx framework captures the distinction between different synchronization scenarios using two RE patterns and exposes them to end-users, independent of MD simulation engine and the resources available.

##### 4.1.1 Synchronous RE Pattern

Synchronous RE pattern depicted in Figure 2.4 (a), corresponds to the scenario where all replicas must finish simulation phase, before any of the replicas can transition to the exchange phase. There is a global synchronization barrier, which forces the replicas arriving at the barrier early to wait for the lagging replicas. Once all replicas are done in the simulation phase all of them transition to the exchange phase. This cycle is then repeated. The synchronous pattern is the conventional way of running REMD simulations, partly because of the implementation simplicity.

### 4.1.2 Asynchronous RE Pattern

Asynchronous RE Pattern, shown in Figure 2.4 (b), does not have a global synchronization barrier between simulation and exchange phase. While some replicas are in the simulation phase, others might be in the exchange phase. Based on some criterion, a subset of replicas transition into the exchange phase, while other replicas continue in the simulation phase. Selection of replicas that will transition may be based on a FIFO principle, e.g. first  $N$  replicas transition into an exchange phase. Alternatively, only replicas which have finished a predefined number of simulation time-steps (2 ps) during some real time interval (1 minute) transition into exchange phase.

## 4.2 Pilot system

The Pilot-Job concept was originally introduced to reduce queue waiting times for workloads on distributed clusters. Pilot-Job systems have been generalized [37] to provide a variety of capabilities, but the two most important are: management of dynamically varying resources and execution of dynamic workloads. A Pilot-Job system supports the execution of workloads with multiple, heterogeneous and dependent tasks[10]. When the placeholder job (pilot) becomes active, it can start executing tasks on acquired computational resources. Resources are available for a duration specified in a job description. Tasks can be submitted for execution before or after the pilot becomes active. Integration of a Pilot-job system in our design enables different RE patterns and number of replicas, independent of the resources available, i.e., supports flexible execution modes, which we now discuss.

## 4.3 Flexible Execution Modes

Decoupling the workload size from the available resources requires: (i) the details of workload be kept separate from the details of resources — type, quantity and availability, and (ii) the ability to execute a workload of a given size (say  $N$  replicas) independent of the specific resources available. As alluded to, Pilot-job systems enable the former; we now discuss how the pilot abstraction allows the latter.

Depending upon the relative size of the resources available ( $R$ ) to the size of simulations ( $S$  = number of replicas  $\times$  resource requirement of each replica), REMD simulations are executed differently. Thus, there are two Execution Modes: when  $R > S$  (Execution Mode I), and when  $R < S$  (Execution Mode II), each of which can be used with any of the two RE patterns.

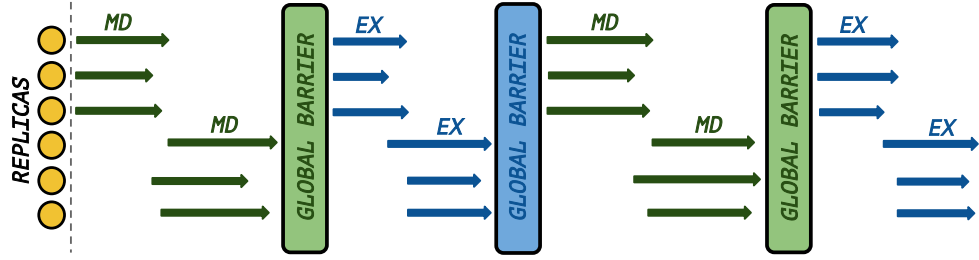


Figure 4.1: Schematic representation of Execution Mode I. On the x-axis is time. Gray squares represent replicas, blue arrows MD phase propagation and green arrows exchange phase propagation. Both MD and exchange phase for all replicas are performed concurrently. After MD and exchange phase is placed a global barrier, ensuring that all replicas enter next phase simultaneously.

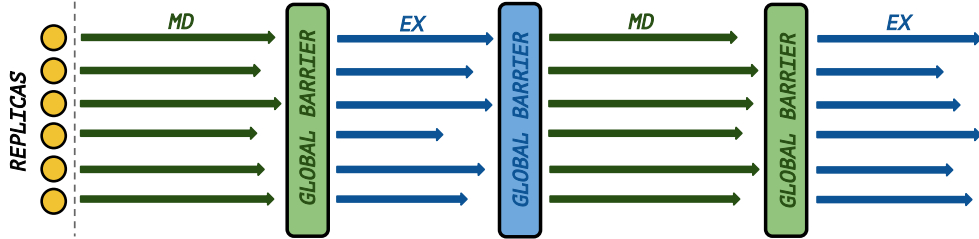


Figure 4.2: Schematic representation of Execution Mode II. On the x-axis is time. Gray squares represent replicas, blue arrows MD phase propagation and green arrows exchange phase propagation. Replicas don't propagate MD and exchange phase concurrently. Batch size for each phase is determined by the number of CPU cores allocated. A global synchronization barrier is present after both MD and exchange phase, ensuring that all replicas enter next phase simultaneously.

#### 4.3.1 Execution Mode I

In Execution Mode I the number of allocated CPU cores satisfies execution requirements of all replicas at a given instant of time. For example, if each replica requires a single CPU core to run, in this mode enough cores are allocated to run all replicas concurrently. Figure 4.1 illustrates capturing Execution Mode I in the context of a Synchronous RE pattern.

#### 4.3.2 Execution Mode II

Execution Mode II supports the scenario when there are not enough CPU cores to run all replicas concurrently. The ratio of cores to replicas is a user defined variable, but typically is a term of a geometric series, e.g.  $\frac{1}{2}$ ,  $\frac{1}{4}$ ,  $\frac{1}{8}$ ,  $\frac{1}{16}$ . As a result, only a fraction of replicas can propagate simulation or exchange phase concurrently. A schematic representation of Execution Mode II is illustrated in Figure 4.2; for simplicity, we depict the synchronous RE Pattern, but Execution Mode II can be used with any of the two available RE Patterns.

While users are given the option to select an execution mode, exact execution details are determined by execution management module of RepEx. The Execution Mode abstraction

hides the gory details of the execution, which differ based upon the relative values of  $R$  and  $S$ . The implementation of Execution Modes vary in the spatial and temporal mapping of workload (tasks) to the allocated CPUs. Specifically, they differ in:

- Order and level of concurrency for task execution
- Number of Pilots used for a given simulation
- Number of concurrently used target HPC resources

Execution Mode is a subset of execution options decoupling simulation requirements from the resource availability and enabling flexible usage of allocated HPC resources. A user should be able to switch between available Execution Modes without any refactoring. In addition to providing conceptual simplicity by hiding details of the execution, Execution Modes provides a significant practical functionality: it permits the study of systems not otherwise possible thanks to the ability to launch more replicas than there are allocatable CPU cores on a target HPC cluster. This might be particularly useful when a user has access to small HPC clusters, but is interested in running REMD simulations involving a large number of replicas. For example, a user can assign as many cores to each replica as needed, or if only a small HPC cluster comprising 128 cores is available user still can perform a simulation involving 10000 replicas.

#### 4.4 Asynchronous RE algorithm

TODO

## Chapter 5

### Implementation

In this chapter we describe the implementation of RepEx. We first present different types of modules available in RepEx. Then we discuss how RepEx is interacting with RADICAL-Pilot to execute its tasks. Next we present a hierarchy of classes and finally we walk through a flow of control in a typical RepEx simulation.

#### 5.1 RepEx Modules

At the core of RepEx are three module types (Figure ??): Execution Management Modules (EMM), Application Management Modules (AMM) and Remote Application Module (RAM).

##### 5.1.1 Execution Management Modules (EMM)

EMMs enable a separation of execution details, namely resource management and workload configuration, from the simulation. Majority of the resource management calls (RP API) are performed in EMM. EMM is responsible for launching a pilot(s) on a target resource, staging-in files at the beginning of the simulation, submission of MD and exchange tasks to a target resource and for the management of the workload dependencies. Due to EMM's ability to encapsulate synchronization routines, each of the two Replica Exchange Patterns is fully specified by a single EMM. Additionally, most of the profiling calls are inserted in EMMs. At the time of this writing in RepEx are available four EMMs:

- **ExecutionManagementModule.** This module is a parent class for all other EMMs. It define a set of attributes common to all EMMs and implements a single function `launch_pilot()`.
- **ExecutionManagementModulePatternS.** This module specifies a synchronous RE pattern. This module is used to run simulations with up to three dimensions with any ordering of these dimensions. Module implements a single function `run_simulation()`.

- **ExecutionManagementModulePatternA.** As the name suggests this module specifies an asynchronous RE pattern. Any number of dimensions is supported by the pattern as well as an arbitrary ordering of exchange types. Module implements a single function `run_simulation()`.
- **ExecutionManagementModulePatternSgroup.** This module is designed to pack replicas belonging to the same group into a single task. Only a synchronous RE pattern is supported by this module.

EMMs are running on the client-side of the RepEx.

### 5.1.2 Application Management Modules (AMM)

AMM is the most complex module of the RepEx. For each supported MD engine is defined a single AMM. AMMs explicitly support *generality* requirement by performing the following operations:

- translation of the user provided parameters to simulation setup
- instantiation of the replicas (replica objects) according to the provided parameters
- management of the simulation input/output files and file movement patterns
- preparation of the Compute Units (tasks) for both simulation phases (MD and exchange)
- exchange of the parameters between replicas
- support of the different exchange types and dimension counts
- support simulation restart from the previous checkpoint in case of failure

Similarly as EMMs, AMMs are running on the client-side of the RepEx.

### 5.1.3 Remote Application Modules (RAM)

As the name suggests modules of this type are running on the server-side (remote system). RAMS are responsible for the following operations:

- generation of individual input files for MD simulation phase
- generation of restraint (.RST) files for MD simulation phase (umbrella exchange)
- calculation of single-point energies (salt concentration exchange)



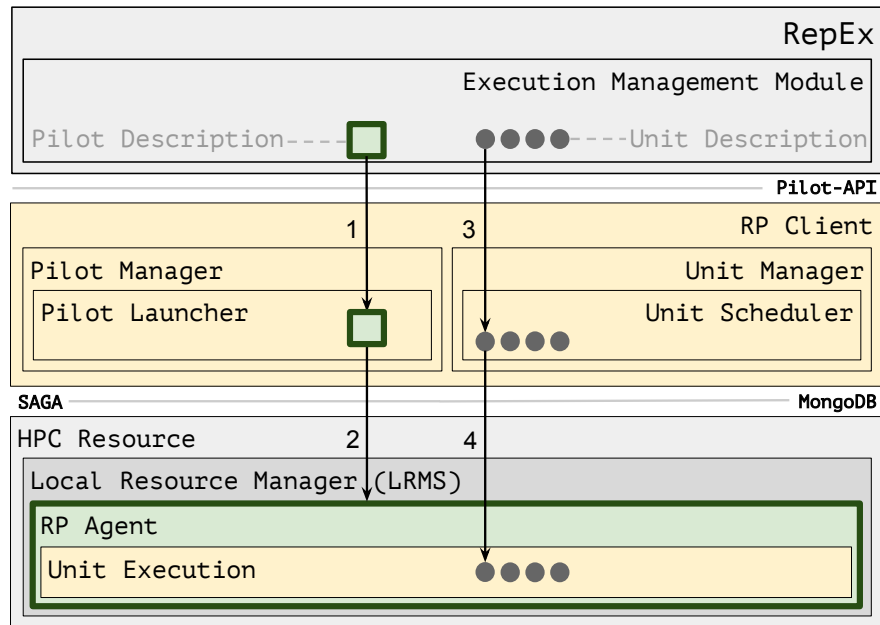


Figure 5.1: RepEx task execution diagram. Top gray square represents RepEx package, middle (yellow) square represents RP API and bottom square represents a target resource. The numbered arrows represent control flow. First in Execution Management Module is created a Pilot description, which is then submitted to RPs Pilot Manager (step 1). Pilot Manager launches a Pilot instance on a target resource (step 2). After a Pilot is active, RepEx workload can be submitted for execution. From Execution Management Module to RPs Unit Manager are submitted Compute Units (step 3), which are defined using a Compute Unit Description. Then Unit Manager submits Compute Units for execution to RPs Agent (step 4).

- reading energy and temperature values from the simulation output files
- performing exchange phase calculations

Due to the differences in formats of input/output files, most of the RAMs are MD engine specific. At the same time most of the exchange calculations are MD engine independent, resulting in reusability of the RAMs. For example, `GlobalExCalculator` module is exactly the same for all MD engines and simulation types, irrespective of the dimension count.

## 5.2 Task Execution Diagram

In Figure 5.1 is presented a diagram showing how RepEx interacts with RADICAL-Pilot to execute its workloads. The gray square on the top of the diagram is RepEx package. Middle yellow square represents RPs API and bottom square an HPC resource. In EMM of RepEx, according to the user provided resource configuration file is created a `Compute Pilot Description`. Then to launch a pilot is performed a call to RPs API (`rp.PilotManager.submit_pilots()`). This call submits a `Compute Pilot Description` to Pilot Manager (step 1), which in turn

launches a pilot (RP Agent) on a target resource (step 2). Once RP Agent becomes active on a resource, it is ready to execute Compute Units (tasks) on allocated CPU cores. Next, from EMM of RepEx for execution are submitted Compute Unit Descriptions (generated according to the user defined simulation input file) to RPs Unit Manager (step 3). These Compute Unit Descriptions can be of any type. Finally, Unit Manager executes these Compute Units on a target resource.

### 5.3 UML Class Diagram

A simplified UML class diagram is presented in Figure 5.3. Execution Management Modules are packaged together in EMMs package (Green square). Application Management Modules can be found in AMMs package (blue square) and Remote Application Modules are organized into two packages - NAMD RAMs and AMBER RAMs (red squares). The only class which does not belong to any package is *Replica* class. These classes are instantiated by AMMs on a client-side of RepEx and are used to record parameters and simulation files associated with a given replica. Any type of REMD simulation requires at least two *Replicas* objects. As mentioned above there are four EMMs in RepEx. The parent class *ExecutionManagementModule*, which implements `launch_pilot()` method and child classes which implement `run_simulation()` method. Child classes must also implement one of the two RE patterns. Between EMMs and AMMs is a uni-directional association: EMMs know about AMMs, but AMMs are not aware of the EMMs. Multiplicity value for this association is 1, since there is a one-to-one mapping between EMM and AMM. Typically only a single instance of EMM and AMM is created during the simulation. A uni-directional association is also between AMMs and RAMs: RAMs are completely self-contained and are not aware of any other classes. All RAMs are instantiated by AMMs. Multiplicity values for association between AMMs and RAMs depend on the class type: RAMs responsible for generation of input files for replica or performing a part of exchange calculations on a per replica basis have multiplicity value of two or more (we must have at least two replicas). Other RAMs, which mainly are responsible for "global" exchange calculations have a multiplicity value of one or more (we have at least one simulation cycle).

### 5.4 UML Control Flow Diagram

We now discuss a control flow in a typical REMD simulation. In Figure 5.4 is depicted a simplified UML control flow diagram for one cycle of the T-REMD simulation with AMBER MD engine. Resource configuration file and simulation input file are passed to a command line tool

replex-amber. Next in replex-amber is created an object of the `ApplicationManagementModuleAmber` class and an object of the `ExecutionManagementModuleS` class. The latter corresponds to a synchronous RE pattern. Next, using an instance of the AMM class, is called a method `initialize_replicas()`, which returns to replex-amber a list of replica objects. After that, to launch a pilot on a target resource, is called `launch_pilot()` method of the EMM. Once a pilot becomes active on a target resource, is called `run_simulation()` method of the EMM. To this method is passed as an argument a list of replica objects and an instance of the AMM class. Within `run_simulation()` method, using an instance of the AMM class is first called a `prepare_shared_data()`. This method populates two lists: `shared_urls` and `shared_files`. The former contains URLs of the simulation input files and the latter the names of these files. These two lists are used to create RPs data directives by both EMM and AMM.

Next is called AMMs function `get_all_groups()`. This function returns a 2D list of replicas grouped according to their group index in a given dimension. Grouping of replicas is important, since part of the exchange phase is performed as a post processing step of the MD phase. We might not have enough CPU cores to launch all tasks concurrently, which can result in a "self-locking" of the simulation. For an exchange phase, replicas depend on the output files of the MD phase generated by the replicas belonging to the same group. If we don't have enough CPU cores to launch all tasks of the MD phase concurrently, we only launch concurrently a subset of groups. Once replicas are grouped, we can prepare tasks for an MD phase.

Now we are ready to prepare Compute Units for the MD phase. Using an instance of the AMM, from the EMM for each replica is called `prepare_replica_for_md()` method, which returns a Compute Unit Description. Once all Compute Unit Descriptions are generated, they are submitted to RPs Unit Manager via `submit_units()` method. Immediately after `submit_units()` in EMM is placed a blocking `wait_units()` call, which returns only after all Compute Units are done.

In this example, execution of each Compute Unit for MD phase has three stages: pre-execution, execution itself and post-execution. At the pre-execution stage is executed `InputFileBuilder` Remote Application Module, which as the name suggests creates AMBER simulation input file (`.mdin`) for a given replica. If exchange type is Umbrella exchange, then for the first simulation cycle this module also creates a restraint (`.RST`) file. At execution stage, is invoked AMBER, which is used to perform a certain number of MD simulation time-steps. Finally, at the post-execution stage is executed `MatrixCalculatorTempEx` RAM. To obtain energy and temperature values for the replicas in the current group, first in this module is called

`get_historical_data()` method. This data is used to calculate reduced energy using a `reduces_energy()` method call. Reduced energy values are used to populate a column of the swap matrix for the given replica.

After all Compute Units of the MD phase are done, can be performed global calculations of the exchange phase. First is called AMMs method `prepare_global_ex_calc()` to prepare a Compute Unit for these calculations. This Compute Unit is then submitted to RPs Unit Manager via `submit_units()` call. After `submit_units()` call is placed blocking `wait_units()` call. Unit Manager executes on a target resource Remote Application Module `GlobalExCalc`. This module performs exchange calculations using Gibbs sampling method and determines pairs of replicas, which should exchange their respective parameters. In `GlobalExCalc` is firsts called `do_exchange()` method, which returns a list of pairs replicas. In `do_exchange()` is called `gibbs_exchange()` method, which for each replica returns a replica to exchange parameters with. `GlobalExCalc` returns `pairs_for_exchange.dat` file in which are written indexes of replicas, which should exchange parameters.

When `GlobalExCalc` is done, in EMM is called `do_exchange()` method of the AMM, which performs an actual exchange of temperatures. At this point a full simulation cycle involving both MD and exchange phases is done. After the whole simulation is done, is called `move_output_files()` method, which moves all files generated in a working directory on the client-side to a single directory called `simulation_output`.

## 5.5 Summary

TODO

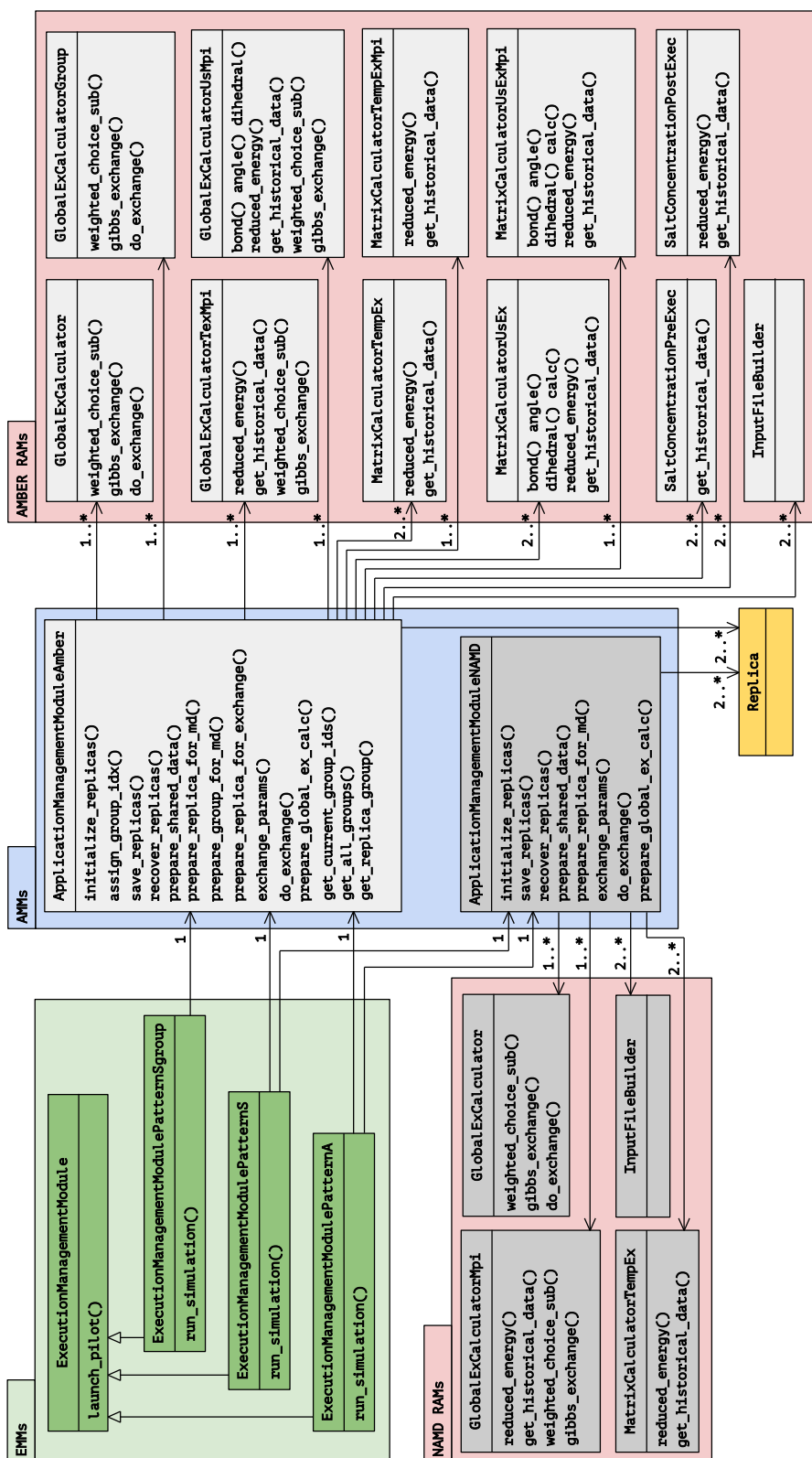


Figure 5.2: UML class diagram. Execution Management Modules are in green boxes. Remote Application Modules are red boxes and Application Management Module is in blue box.

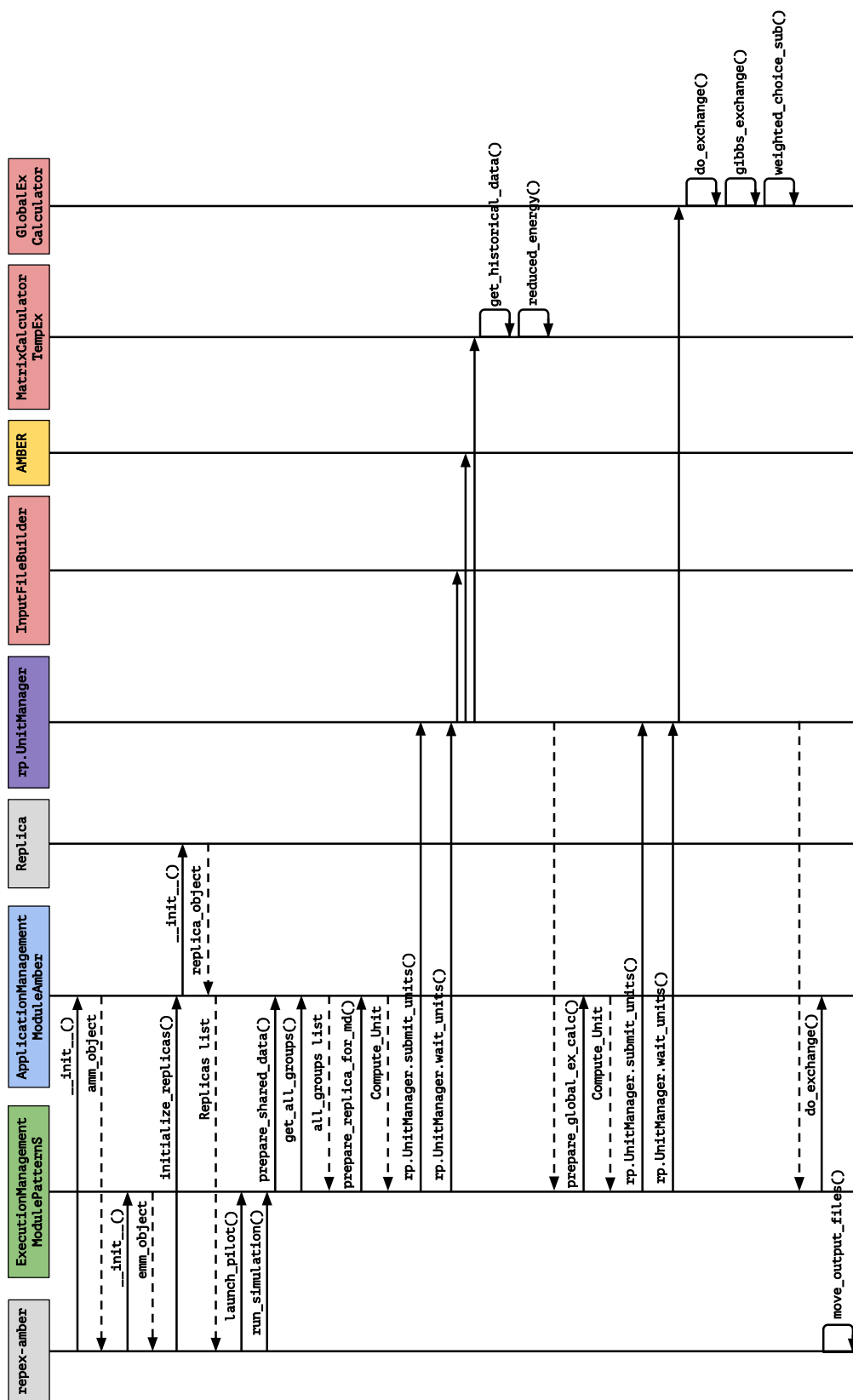


Figure 5.3: UML Control Flow Diagram.

## Chapter 6

### Validation

In this chapter we validate implementation of RepEx. 3D-REMD was performed using order parameters of temperature, and umbrella sampling in the  $\phi$  and  $\psi$  torsion angles (as shown in Figure 6.1). In the temperature (T) dimension, six windows were chosen from 273K to 373K by geometrical progression. In both umbrella (U) dimensions, eight windows were selected uniformly between  $0^\circ$  and  $360^\circ$ , where each window corresponds to a harmonic restraint centered on it with a force constant of  $0.02 \text{ kcal}\cdot\text{mol}^{-1}\cdot\text{degree}^{-2}$ . The total number of replicas is therefore  $6\times 8\times 8=384$ . Each replica was previously equilibrated for  $> 1 \text{ ns}$ . In the production run, we set the exchange attempt interval (cycle) to be 20000 steps (20 ps) and in a 15-hour run with 400 cores (25 nodes) on Stampede [38], the simulation finished 90 cycles (1.8 ns). The acceptance ratios of exchange attempts are approximately 3% for T dimension and 25% for U dimensions. Free energy profiles were then generated from the last 1 ns of production data using the maximum likelihood approach implemented in the vFEP package [39, 40]. Free energy profile of the alanine dipeptide system along the  $\phi$ - $\psi$  angles has been studied extensively by theoretical and experimental methods. Figure 6.1 demonstrates identical free energy profiles at 300K, compared with other recent computational studies [? ], [? ]. The enthalpy contribution of  $\alpha R/c7_{eq}$  transition has not been reported in any computational studies. Nevertheless, the temperature dependency of free energy profiles in Figure 6.1 has been utilized to estimate this enthalpy contribution as 1.2 kcal/mole, comparable to the known experimental reported value 1.1 kcal/mole. [? ]

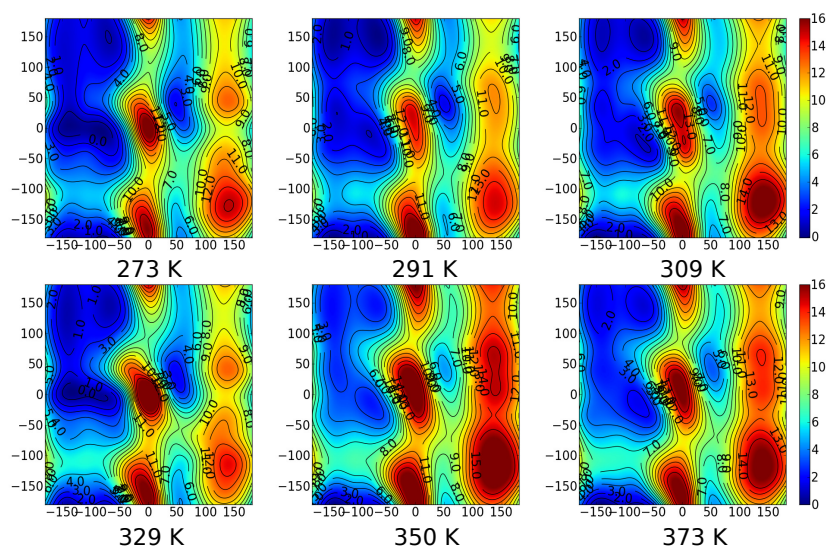


Figure 6.1: Free energy profile of alanine dipeptide backbone torsion at six different temperatures. In all six subplots, the x and y-axes correspond to  $\phi$  and  $\psi$  torsion angles, respectively. The range of energies is from 0 kcal/mol to 16 kcal/mol while each level in the contour corresponds to a 1 kcal/mol increment.



## Chapter 7

### Performance Optimization

#### 7.1 Initial Evaluation

To evaluate our initial implementation we perform 3D REMD simulation runs using Amber as MD engine on Stampede. We use TUU-REMD simulation, comprising one temperature dimension and two umbrella sampling dimensions. For all experiments, we measure and plot average REMD simulation cycle time, which is an average of 4 simulation cycles. Experiments were performed using alanine dipeptide (Ace-Ala-Nme) solvated by water molecules and comprising 2881 atoms. In all three dimensions we perform 6000 time-steps between exchanges, which takes on average 136.64 seconds (in each dimension). Order of dimensions is fixed: umbrella sampling exchange is followed by temperature exchange, which is followed by second umbrella sampling exchange. For all simulation runs, we use the Synchronous RE pattern and Execution Mode I: number of CPU cores is greater or equal to the number of replicas, meaning that all replicas propagate both simulation and exchange phases concurrently. For initial experiments, number of replicas in each dimension is equal, which results in the total number of replicas being a number raised to the power of three. We use RADICAL-Pilot 0.33 and sander as Amber executable.

**Input files:** For our experiments parameters (file extension .prmtop) and coordinates (file extension .inpcrd) files are shared between all replicas, meaning that only a single instance of each file needs to be transferred from local system to Stampede. It is important to note, that for certain simulation types, each replica may require an individual coordinates file. Amber input files (file extension .mdin) are generated locally for each replica and then transferred to Stampede. This is done for each MD cycle in each dimension. For alanine dipeptide these files are 334 bytes large. For umbrella exchange, locally are generated Amber restraint files (file extension .RST) and transferred from local system to Stampede once, at the beginning of the simulation. Each of these files is 213 bytes in size.

**Output files:** During the exchange phase each of the replicas generates a `matrix.column.d.c.dat` file. Size of this file depends on the number of replicas used for a given simulation: for 64 replicas run file size is 331 bytes, for 216 replicas run file size is 962 bytes, for 512 replicas run size is 2.2 Kilobytes. After exchange is finished, these files are transferred from Stampede to laptop for final processing. This is done for each dimension and for each simulation cycle. Pairs of replicas for exchanges of parameters are determined locally.

For M-REMD simulations,  $T_c$  is comprised of the 1D cycle time for each dimension, since simulations are performed only in one dimension at any given instant of time.

Initially we define a simulation cycle time as:

$$T_c = T_{MD} + T_{EX} + T_{data-init} + T_{data} + T_{RepEx-over} + T_{RP-over} \quad (7.1)$$

where:

- $T_{MD}$  - MD simulation time, time to perform X simulation time-steps
- $T_{EX}$  - Exchange time. Time for calculations required to determine exchange partners
- $T_{data}$  - Data time. Time to perform data movement procedures, which are mostly remote-to-remote. For example, Amber's `.mdinfo` files to "staging area" which is accessible by subsequent tasks
- $T_{data-init}$  - Initial data transfer to the remote system. Time required to transfer files required to as inputs for MD phase and Exchange phase from local system to remote system (HPC cluster). Note: initial data staging is performed once per simulation and not for every cycle.
- $T_{RepEx-over}$  - RepEx overhead. Time to prepare tasks for execution and time to perform local RepEx method calls
- $T_{RP-over}$  - RP overhead. Time required for task launching on a target resource and time for internal RP communication

Initial performance results are presented in Figure 7.1. For all three runs, MD times are less than 50 % of the cycle time. For simulation run with 64 replicas, MD time comprises  $\sim 35$  % of the cycle time, for the run with 216 replicas  $\sim 16$  % and for the run with 512 replicas  $\sim 7$  %. All timings, with exception of MD simulation time demonstrate exponential growth. As seen in Figure 7.1, for all three runs, initial data staging takes a significant amount of time. For experiment with 512 replicas, initial data stagingn takes around 550 seconds, which is sub-optimal.

Clearly, there is a lot of potential for performance improvement. In the next section we outline and present our performance optimization strategy.

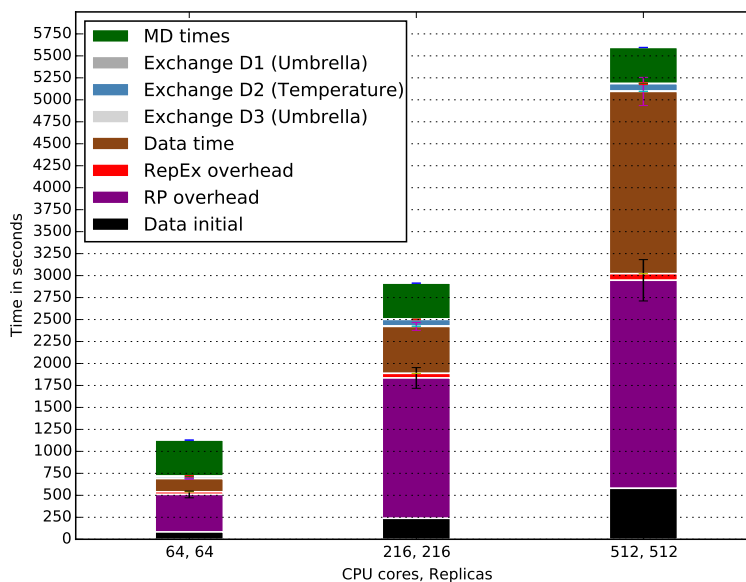


Figure 7.1: Initial performance results: Decomposition of average simulation cycle time into contributing factors for alanine dipeptide TUU-REMD. All simulation runs are performed on Stampede.

## 7.2 Optimization I

As a first performance optimization step, we reduce time required for data movement. We eliminate the need to transfer from local system to remote HPC cluster, simulation input files (.mdin) for each replica. Instead, we transferring a single, shared input file template and a script which generates an input file for each replica according to specified simulation parameters. This means that we need to add a pre-execution step for MD simulation tasks, which would run the script to generate simulation input file for each replica. In input file template, parameters specific to individual replica are substituted with placeholders. A script substitutes placeholders in input file template with parameters corresponding to a given replica. This procedure occurs at a pre.exec (pre-execution) stage of a Compute Unit. For each cycle and in each dimension we generate simulation input file on a remote HPC cluster (Stampede).

Performance results of this optimization are presented in Figure 7.2. As depicted in Figure 7.2, this optimization resulted in substantial decrease in data times and RP overhead times. All other timings remained the same. RP overhead timings were reduced, since task launching delay is affected by the number and size of files which are staged-in prior to task execution. Data time for simulation run with 64 replicas is now reduced by  $\sim 70$  seconds, but RP overhead time by  $\sim 190$  seconds. For run with 216 replicas, performance gains are more apparent. Data time decreased by  $\sim 240$  seconds, but RP overhead by  $\sim 1280$  seconds. Lastly, for the run with

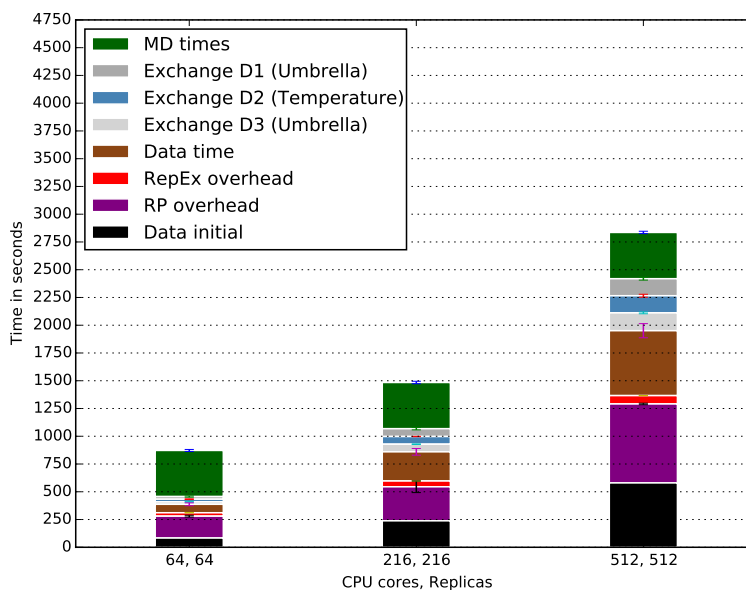


Figure 7.2: Optimization I: remote generation of simulation input files. Decomposition of average simulation cycle time into contributing factors for alanine dipeptide TUU-REMD. All simulation runs are performed on Stampede.

512 replicas, data time was reduced by  $\sim 1400$  seconds and RP overhead by  $\sim 1380$  seconds.

### 7.3 Optimization II

To further reduce time for file staging, we eradicate transferring of restraint (.RST) files for umbrella exchange dimensions. Similarly as with simulation input files, from the local system we transfer to remote HPC cluster only a restraint file template and a script, which generates restraint file based on provided parameters. Both, restraint file template and a script are shared among all replicas. In restraint file template, parameters specific to individual replica are substituted with placeholders. Before first simulation cycle, each task (RP's Compute Unit) runs a script, which substitutes placeholders in restraint file template with parameters corresponding to a given replica. This procedure is performed only once and is specified as a pre\_exec (pre-execution) stage of a Compute Unit. As a result, we create all restraint files on a remote cluster and don't need to transfer all of the from local system.

In addition, we also reduce the number of file transfers for the exchange phase. Previously, for exchange, we transferred  $N$  (number of replicas) `matrix_column.d.c.dat` ( $d$  is dimension,  $c$  is cycle) files, from remote cluster to local system to finalize exchange phase. Now we determine exchange partners remotely, thus eliminated the need to transfer  $N$  `matrix_column.d.c.dat`

files. As a result we transfer a single file with replica ids. During the exchange phase, when all individual exchange tasks are complete, we execute an additional task (Remote Application Module), which reads data from individual `matrix_column_d.c.dat` files and determines pairs of replicas for exchange of parameters.

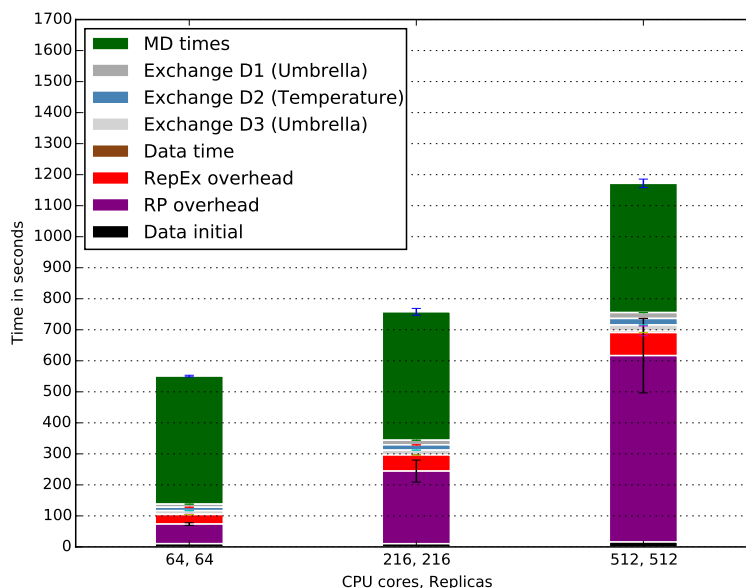


Figure 7.3: Optimization II: remote generation of restraint files and remote determination of exchange partners. Decomposition of average simulation cycle time into contributing factors for alanine dipeptide TUU-REMD. All simulation runs are performed on Stampede.

Resulting timings are provided in Figure 7.3. Intuitively, the aforementioned optimizations allowed to reduce initial data time and data time. All other timings were not affected by this optimization. The initial data times decreased by 71, 235 and 508 seconds for simulations involving 64, 216 and 512 replicas respectively. Due to elimination of restraint file transfers from local system to remote cluster, initial data times are now independent of replica counts and take  $\sim 12$  seconds for all three runs.

Elimination of `matrix_column_d.c.dat` file transfers, resulted in substantial decrease in data times. For a simulation run with 512 replicas, data times decreased by  $\sim 510$  seconds.

## 7.4 Optimization III

Analysis of the Compute Unit execution profiles, revealed that there is a considerable delay between execution start-up times of the Compute Units. Despite being submitted for the execution simultaneously, Compute Units will not start executing at the same time. In addition, as

the number of simultaneously submitted Compute Units increases, difference between execution start of the first unit and execution start of the last unit, is increasing proportionally to the number of units.

In RepEx, for both MD and exchange phases we create a separate set of Compute Units, which is equal in size to the number of replicas. To mitigate the effect of the execution start-up delay of RP's Compute Units, we merge MD phase units with exchange phase units. As a consequence, exchange phase tasks now are performed as a post-execution (`post_exec`) step of the MD compute units.

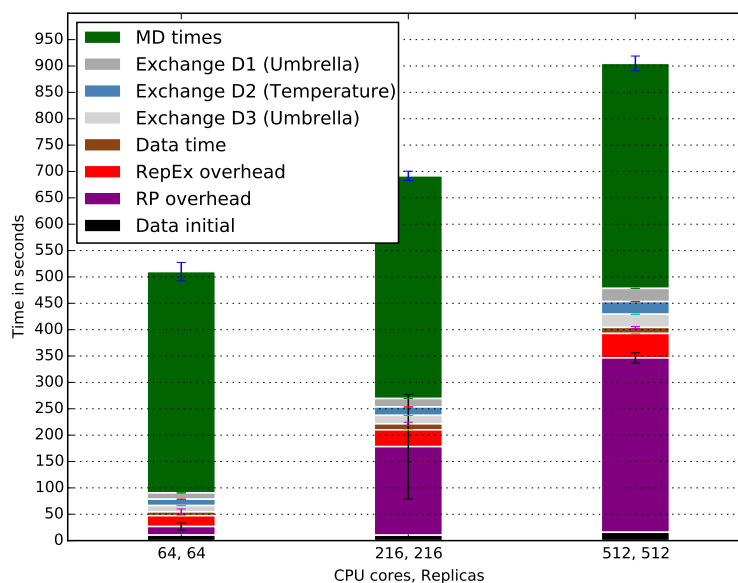


Figure 7.4: Optimization III: merging of MD simulation tasks with exchange tasks. Decomposition of average simulation cycle time into contributing factors for alanine dipeptide TUU-REMD. All simulation runs are performed on Stampede.

Average simulation cycle times after optimization III are shown in Figure 7.4. As shown in Figure 7.4, RP overhead times decreased for all three runs. For the run with 64 replicas, RP overhead decreased by 58 seconds. For simulation run with 216 replicas, by *sim*90 seconds and for the run with 512 replicas, by *sim*270 seconds.

Execution start-up delay for Compute Units, currently is the largest contributing factor to the simulation overhead. In ideal case, MD time should be responsible for the *sim*90% of the average REMD simulation cycle time. Currently, for the run with 512 replicas, MD time is responsible for *sim*47% of the total simulation cycle time, despite the fact, that we have reduced execution start-up delay for nearly a half for all runs.

## 7.5 Optimization IV

All simulation runs for optimizations I,II and III were performed using default configuration of RADICAL-Pilot agent. It is possible to modify this configuration by increasing a number of execution and data staging workers, thus improving the performance of the application. Experimentally it was determined that for the Stampede cluster the best configuration is with 8 components for each of the workers. In addition, we now are using a development branch of the latest RADICAL-Pilot version (v0.42-143-gcefb3b@devel).

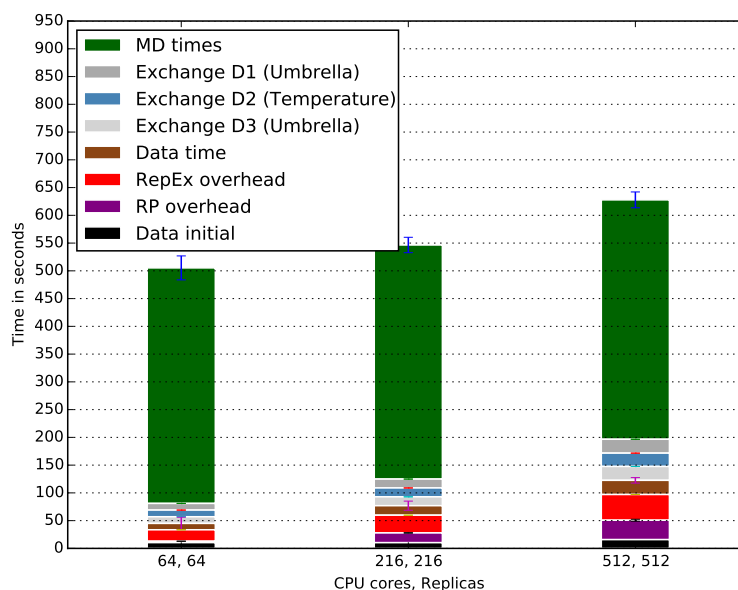


Figure 7.5: Optimization IV: Increasing the number of execution and data staging workers for RP agent. Using a development branch of the latest RP version. Decomposition of average simulation cycle time into contributing factors for alanine dipeptide TUU-REMD. All simulation runs are performed on Stampede.

In Figure 7.5 are presented results after making the above changes. As we can see, for all three runs we achieved a substantial decrease in RP overhead: for simulation run involving 216 replicas, RP overhead is now reduced by  $\sim 140$  seconds, but for the run with 512 replicas by  $\sim 290$  seconds.

## 7.6 Optimization V

To further decrease RP overhead, RepEx overhead, Data times and exchange times, we decided to merge multiple MD and exchange tasks into a single Compute Unit. We merge together only tasks which are belonging to the same group in the current exchange dimension. More

information on grouping of replicas for multi-dimensional REMD simulations can be found in section 2.6. For a simulation involving 1000 replicas, this approach allows to reduce the number of tasks by a factor of 10.

To merge MD and exchange tasks for multiple replicas into a single Compute Unit for each exchange type we write a special Remote Application Module. This module is a Python MPI script, which is responsible for creation of simulation input files, restraint files, concurrent execution of Amber executables and exchange calculations.

This approach also substantially reduces the number of I/O operations, since for a group of size  $N$ ,  $N$  files are read now by a single script, instead of by  $N$  scripts.

One major drawback of this approach is that it only can be used for MD tasks requesting a single CPU core. This means that if we are using Amber, we can't use `pmemd.MPI` or `pmemd.cuda`.

Unfortunately, we were not able to achieve consistent performance improvements for this optimization. There are two reasons for that. First, performance of MPI tasks launched by RP, when the number of requested CPU cores is less than one node is inconsistent. Second, launching of MPI Compute Units by RP is slower than launching of single core Compute Units. Nevertheless, we believe that when the aforementioned problems will be resolved, this optimization might be useful.

## 7.7 Summary

TODO



## Chapter 8

### Experiments

Having validated both the design and implementation of RepEx, in this section we discuss a series of experiments used to demonstrate the unique functional capabilities and characterize its performance.

For all experiments, we measure and plot the average REMD simulation cycle time, which is an average of 4 simulation cycles. Experiments were performed using alanine dipeptide (Ace-Ala-Nme) solvated by water molecules on Extreme Science and Engineering Discovery Environment [38] (XSEDE) allocated systems: Stampede and SuperMIC. For all experiments was used Synchronous RE pattern.

Simulation cycle time is calculated using formula defined in section 7.1. For M-REMD simulations,  $T_c$  is comprised of the 1-D cycle time for each dimension, since simulations are performed only in one dimension at any given instant of time.

We calculate weak scaling efficiency as:

$$E_w = \frac{T_1}{T_N} \times 100\% \quad (8.1)$$

where:

- $T_1$  - time to complete simulation cycle involving minimal number of replicas  $R_{min}$  with number of CPU cores equal to the number of replicas, e.g. 8 replicas on 8 CPUs
- $T_N$  - time to complete simulation cycle involving  $N$  replicas with  $N$  CPU cores

We calculate strong scaling efficiency as:

$$E_s = \frac{T_1}{(M/N_{min}) \times T_N} \times 100\% \quad (8.2)$$

where:

- $T_1$  - time to complete simulation cycle involving  $N$  replicas with minimal number of CPU cores  $N_{min}$ , e.g. 1024 replicas on 8 CPUs
- $T_N$  - time to complete simulation cycle involving  $N$  replicas with  $M$  CPU cores, where  $N_{min} < M$
- $M$  - number of used CPU cores

Results obtained in Section ?? can be reproduced by following instructions at [41]. All experiments were performed with RP version 0.35. Last version of RP is 0.40.1 and thanks to various optimizations it is capable of substantially better performance. These optimizations, however, only alter the RP overhead timings (as well as data timings) presented in this section and will have minimal impact on the overall performance characterization of RepEx.

## 8.1 Characterization of Overheads

There are three factors which contribute to the  $T_c$  as a result of design decisions we have made. These factors are data time, RepEx overhead and RP overhead. In this subsection, we summarize how these factors influence the  $T_c$ .

Figure 8.1 presents the values of data times, RepEx overheads and RP overheads for simulation runs involving 64, 216, 512, 1000 and 1728 replicas on SuperMIC. For all runs, we use a single CPU core per replica and use Execution Mode I with synchronous RE pattern.

Values of data times depend on the exchange type, since data movement patterns differ for each exchange type. As depicted in Figure 8.1, data times for temperature exchange are shorter than for umbrella exchange and salt concentration. For all replica counts, data times are relatively small: longest data transfer time is 6.3 seconds. This is due to the fact, that majority of the transfers are happening within the cluster/resource. Consequently, data times change as a function of a target system, since largest contributing factor, is the performance of a parallel file system.

RepEx overhead depends on the total number of replicas and on simulation type. For all 1D simulations, values of RepEx overhead are nearly identical, since the number of operations to perform task preparation is very similar. RepEx overhead times for 3D simulations are longer, since there are more data associated with each replica, complexity of data structures is increased and more computations are performed during task preparation.

RP overhead depends only on the number of replicas (tasks) launched concurrently. As we can see in Figure 8.1, RP overhead is proportional to the number of replicas.

## 8.2 Performance Characterization of 1D-REMD

In this subsection, we characterize performance of 1D REMD simulations with RepEx. For each of the three available 1D-REMD simulations: temperature exchange (T-REMD), umbrella exchange (U-REMD) and salt concentration exchange (S-REMD) we measure average cycle times. We perform simulation runs involving 64, 216, 512, 1000 and 1728 replicas in Execution

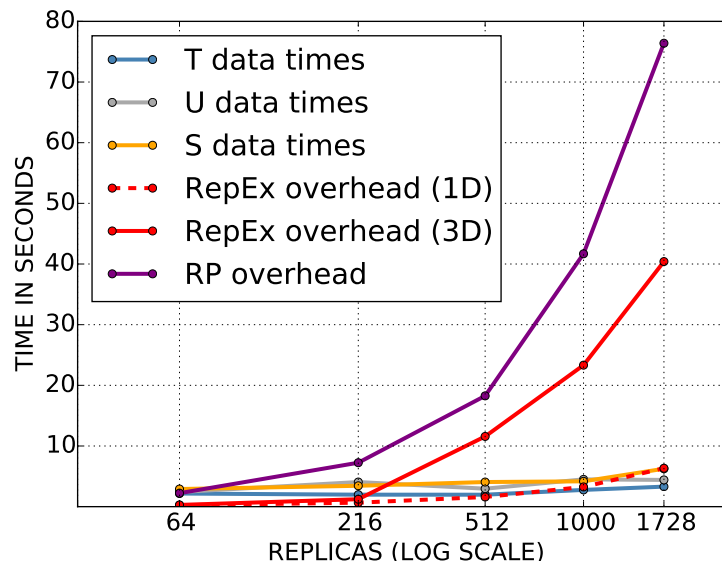


Figure 8.1: Characterization of overheads: Data times, RepEx overhead and RP overhead.

Mode I. All runs are conducted with a single CPU core per replica and **sander** as the Amber executable. We use alanine dipeptide solvated by water molecules comprising a total of 2881 atoms and perform 6000 simulation time-steps between exchanges. We perform all runs on SuperMIC supercomputer [38]. Results of these experiments are presented in Figure 8.2.

As we can see, for all three exchange types, the time to perform 6000 time-steps is nearly identical, as evidenced by the almost similar average heights of dark green bars in Figure 8.2 (139.6 seconds).

Next we discuss exchange timings for different exchange parameters, as seen in the lower panel of Figure 8.2. Timings for temperature and umbrella exchange are similar and have a nearly linear growth rate. For both exchange types, we use a single MPI task to perform an exchange. In case of U-REMD we have implemented a single point energy calculation internally. Despite the fact that U-REMD exchange is more involved, we don't see a significant difference in exchange timings between U-REMD and T-REMD.

Due to the mathematical complexity, the single point energy calculation for S-REMD is calculated using Amber for each replica in each state. This implies that for each replica, an additional task is required. Since we are using Amber's group files, this task requires at least as many CPU cores as there are potential exchange partners for each replica. Consequently, the exchange times for S-REMD are substantially longer, but nonetheless have a nearly linear growth rate.

The parallel efficiency results for the 1D-REMD simulations are presented in Figure 8.3.

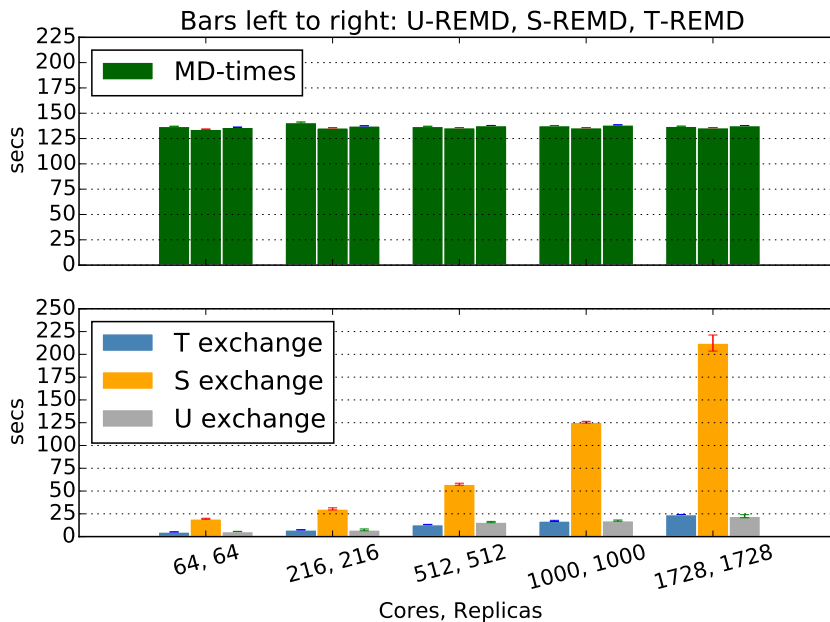


Figure 8.2: 1D REMD experiments with RepEx: weak scaling. Decomposition of average simulation cycle times  $T_c$  (in seconds) into MD simulation time and exchange time for umbrella sampling, salt concentration and temperature exchange. For all simulation runs the number of replicas is equal to the number of CPU cores (e.g. 1 core per replica) and both vary from 64 to 1728. All simulation runs are performed on SuperMIC supercomputer.

We calculate parallel efficiency for the weak scaling scenario and use average cycle time for simulation with 64 cores as starting point, e.g. 100% efficiency. We also present efficiency results for simulations without an exchange phase (black line). This quantifies the influence of exchanges on the efficiency of 1D simulations. Since all tasks have overheads associated with them, we observe a decrease in efficiency even if there is no exchange. For all three exchange types we observe decrease in efficiency while increasing the number of cores. Efficiency values for T-REMD and U-REMD are similar and demonstrate linear behavior. Efficiency for S-REMD is lower. This is caused by specifics of exchange phase, discussed earlier.

### 8.3 T-REMD with NAMD engine

To demonstrate RepEx's ability to use different MD engines for REMD simulations we perform weak scaling experiments using T-REMD with NAMD engine. We run our experiments on SuperMIC, use NAMD-2.10 and perform a total of 4000 time-steps between exchanges. We perform runs with 64, 216, 512, 1000 and 1728 replicas. For each replica we use a single CPU core and we allocate enough cores to run all replicas concurrently (Execution Mode I). Results of these experiments are provided in Figure 8.4.

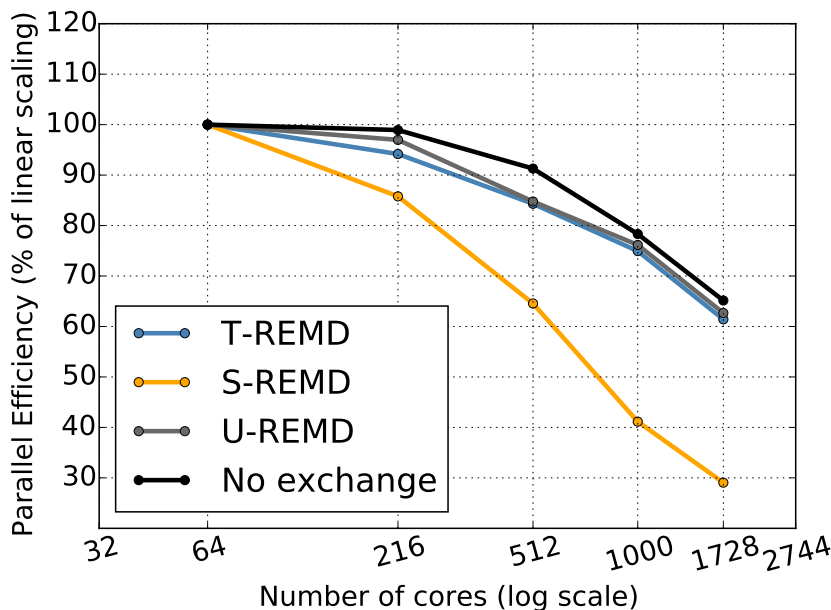


Figure 8.3: Parallel Efficiency (% of linear scaling) for Temperature Exchange REMD (1D), Salt Concentration REMD (1D) and Umbrella Sampling REMD (1D) using Amber MD engine on SuperMIC supercomputer.

As expected, MD times for all cores/replicas pairs are nearly equal. The growth rate for exchange times can't be characterized as monomial.

#### 8.4 M-REMD performance characterization

Similar to 1D-REMD experiments, we use alanine dipeptide to characterize M-REMD performance and 6000 simulation time-steps between exchanges. We perform weak and strong scaling experiments for TSU-REMD on Stampede.

**Weak Scaling:** To characterize the weak scaling performance of M-REMD simulations, the number of replicas in each dimension is kept equal, thus, as the number of replicas in one dimension varies from 4, 6, 8, 10 and 12, it results in the total number of replicas equal to 64, 216, 512, 1000 and 1728 respectively. We use Amber 12.0, and **sander** as Amber executable, as for each replica we use a single CPU core. The experiments are performed in Execution mode I, i.e., with enough cores to run all replicas concurrently. Results of experiments are provided in Figure 8.5.

For all simulation runs MD times are nearly identical:  $\sim 495.0$  seconds. It is expected, since variation in the number of replicas should not affect MD time.

We observe a nearly linear scaling for exchange timings in all three dimensions. While

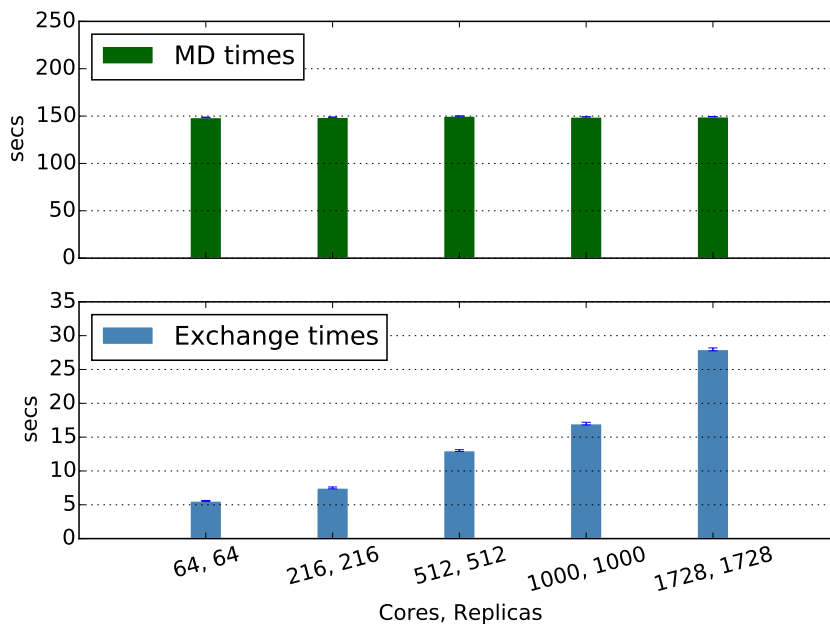


Figure 8.4: Experiments with NAMD engine. Decomposition of average simulation cycle times  $T_c$  (in seconds) into MD simulation time and Exchange time for weak scaling scenario. Experiments are performed on SuperMIC supercomputer, using T-REMD. For MD simulation are used single-core replicas.

temperature and umbrella exchange timings are very similar, salt concentration exchange takes substantially more time. As mentioned in Subsection 8.2, for salt concentration exchange we use Amber to perform a single point energy calculations, which results in doubling of tasks and higher computational requirements for this exchange type.

Parallel Efficiency results are presented in Figure 8.7(a). We observe a rapid decrease in efficiency with increase in the number of cores. This can be explained by the influence of performance for salt concentration exchange. Despite that, for all core counts, efficiency is above 50 %.

**Strong Scaling:** To characterize the strong scaling performance of M-REMD RepEx, the number of replicas is fixed at 1728 with 12 replicas in each dimension, but the number of cores is varied: 112, 224, 432, 864 and 1728. Again, we use Amber 12.0, and **sander** as Amber executable, since for each replica a single CPU core is used. The experiments are performed using Execution Mode II, as we have fewer cores than replicas for all cores/replicas pairs, except the last one. Results of these experiments are provided in Figure 8.6.

As illustrated in Figure 8.6, decrease in MD time is proportional to the number of cores: the doubling of the number of CPU cores, results in decrease of MD time by nearly a half.

Exchange time in temperature exchange and umbrella exchange dimensions is almost equal

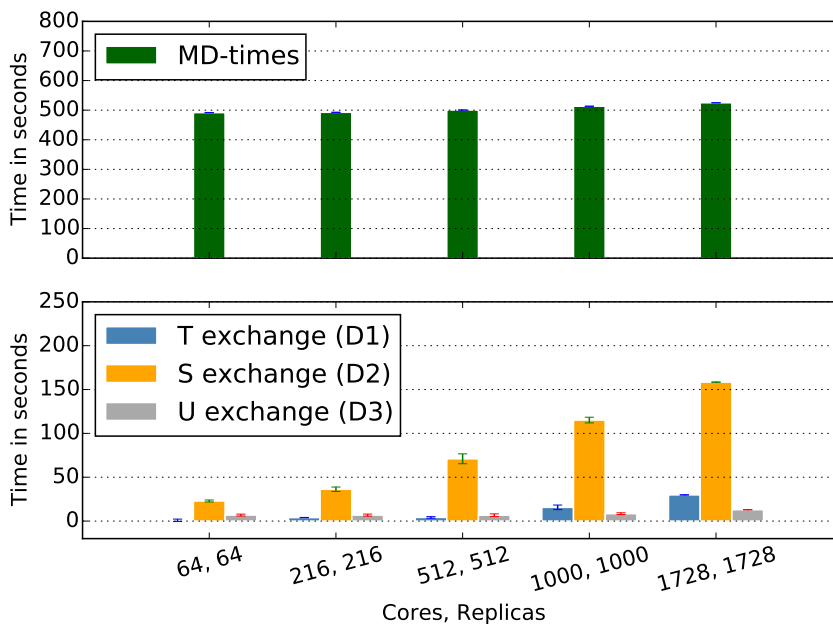


Figure 8.5: Multi-dimensional REMD experiments with RepEx - weak scaling. TSU-REMD on Stamped using Amber MD engine. For all simulation runs the number of replicas is equal to the number of CPU cores and both vary from 64 to 1728. For all simulation runs are used single-core replicas. In figure is shown decomposition of average simulation cycle times  $T_c$  (in seconds) into MD and exchange times.

for all numbers of CPU cores. This highlights the fact, that implementation of temperature exchange and umbrella exchange are very similar. Due to task launching delay and grouping of replicas by parameter values in each dimension, the exchanges largely overlap with MD. As a result, tasks which have finished simulation phase sooner can perform certain exchange procedures, before an exchange is finalized. Compared to temperature exchange and umbrella exchange, salt concentration exchange times are significantly higher: at 112 cores, salt exchange time takes nearly 1800 seconds.

Parallel Efficiency results are presented in Figure 8.7(b). As we can see, efficiency graph is non-linear. We observe a decrease in efficiency up to the last data point where number of CPUs is equal to the number of replicas. For the last data point, efficiency increases. This behavior is caused by the MPI task scheduling issue of RP. In the next release of RepEx this issue will be addressed.

## 8.5 REMD with Multi-core Replicas

To demonstrate RepEx's capability to execute replicas using multiple CPU cores we use solvated alanine dipeptide with 64366 atoms. We perform a total of 20000 time-steps between each

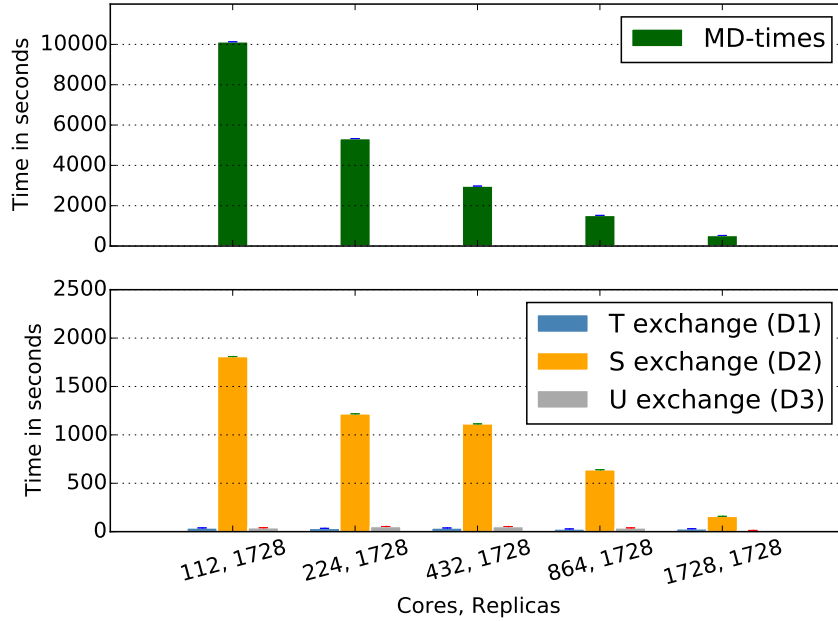


Figure 8.6: Multi-dimensional REMD experiments with RepEx: strong scaling. TSU-REMD on Stampede using Amber MD engine. Number of replicas is fixed at 1728, but the number of CPU cores is increased from 112 to 1728. For all runs are used single-core replicas. In figure are shown MD simulation and exchange times. RepEx enables users to vary the size of computational resources independently of the simulation size. Allocating more CPUs reduces the  $T_c$ .

exchange. Experiments are performed on Stampede using Amber 12.0 and pmemd.MPI as Amber executable for multi-core replicas and sander for single-core replicas. We use different executables, since pmemd.MPI can't be run on a single CPU core.

We perform weak scaling experiments using multi-core replicas and multi-dimensional TUU-REMD with one temperature dimension and two umbrella dimensions. We perform simulation runs with fixed number of replicas and change number of CPU cores per replica. For all runs, we use 216 replicas, but the number of cores per replica varies from 1 to 64. Results of these experiments are provided in Figure 8.8.

We observe a substantial drop in MD times when we use multiple cores per replica. We attribute this drop due to RepEx's ability to support replicas running over multi-core/multi-nodes, as well as using a highly efficient pmemd.MPI code. Further increase of CPU cores per replica doesn't demonstrate a linear behavior. This is not a limitation of the RepEx framework but attributable to the size of the alanine dipeptide, which although relatively larger than the earlier physical system, is small in absolute terms and thus makes it difficult to gain significant performance improvements by using more CPUs.



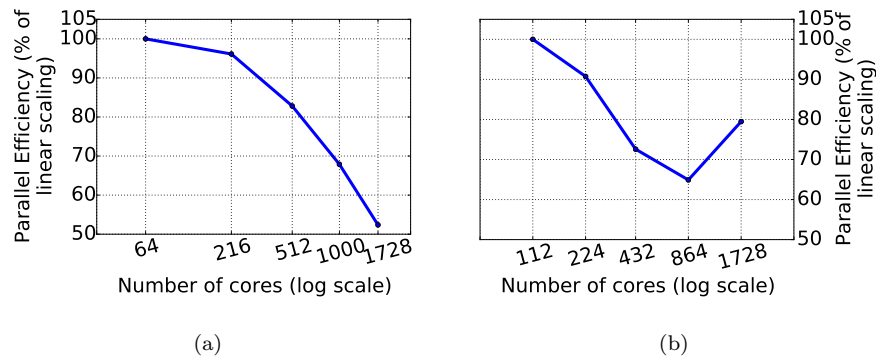


Figure 8.7: Parallel Efficiency (% of linear scaling) for TSU-REMD on Stampede using Amber MD engine - (a) weak scaling, (b) strong scaling.

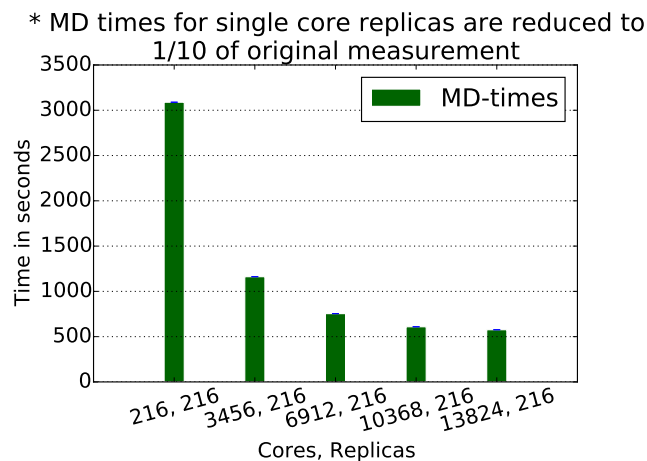


Figure 8.8: Multi-core replica experiments using TUU-REMD with Amber engine. MD times for weak scaling scenario. Experiments are performed on Stampede supercomputer. Number of replicas is fixed at 216, but the number of CPUs per replicas is increased from 1 to 64.

## 8.6 Asynchronous REMD

This section is aimed at identification and quantification of advantages and disadvantages associated with the use of asynchronous RE pattern. First, we compare and contrast synchronous and asynchronous RE patterns in terms of resource utilization. Next, we quantify the differences in exchange metrics, such as crosswalks, accepted exchanges and attempted exchanges between the two patterns.

### 8.6.1 Resource Utilization

First, we compare resource utilization for synchronous and asynchronous RE pattern. For both patterns we use TUU-REMD with Amber MD engine. We run a Quantum mechanics

/ Molecular Mechanics (QM/MM) simulation with a truncated dinucleotide molecule. We simulate a non-enzymatic transesterification reaction, which is a model reaction for the RNA cleavage reaction. The QM method we are using is called AM1/d-PhoT which is a semi-empirical method that is specially parametrized for this type of reaction.

We calculate resource utilization as:

$$U = \frac{U_{pattern}}{U_{max}} \times 100\% \quad (8.3)$$

where:

- $U_{pattern}$  - utilization using (async/sync) RE pattern. Total simulation time obtained on  $N$  CPU cores.
- $U_{max}$  - maximal (ideal) utilization, when we run MD on all allocated CPU cores 100% of the time.

In RepEx interaction with Amber MD engine (or any other MD engine) is done through Amber input/output files. Thus, it is imperative to understand by how much a shared file system of a given HPC cluster affects performance of RepEx and how the role of a file system changes at scale.

We perform all simulation runs on Stampede HPC cluster. For all runs we use a single CPU core per replica and each run is 240 minute long. To demonstrate fluctuation in execution times of MD tasks, we perform weak scaling runs with 216, 512, 1000 and 1728 replicas while simulating 2000 time-steps in between exchanges. Obtained results are presented in Figures 8.9, 8.10, 8.11 and 8.12 respectively.

In Figure 8.9 are plotted execution times for MD Compute Units, as they are measured internally by Amber and execution times together with file staging times as they are measured by RP profiler. For the first 216 Compute Units timings with file staging (red line) are much higher, then for the rest of the units. This can be explained by the setup of the shared file system on Stampede. For the rest of the units file staging times on average are *sim*6 seconds. As we can see, difference in execution times between MD Compute Units can be up to 100 seconds. Another observation is increase in execution times for units 3000-3216. This can only be explained by the system noise at the time of the measurement.

Similar results were obtained for simulation run with 512 replicas (Figure 8.10). For the first 512 Compute Units file staging times are longer, than for the rest of the units. On average file staging times are still relatively short, but difference in execution times does not exceed 100 seconds.

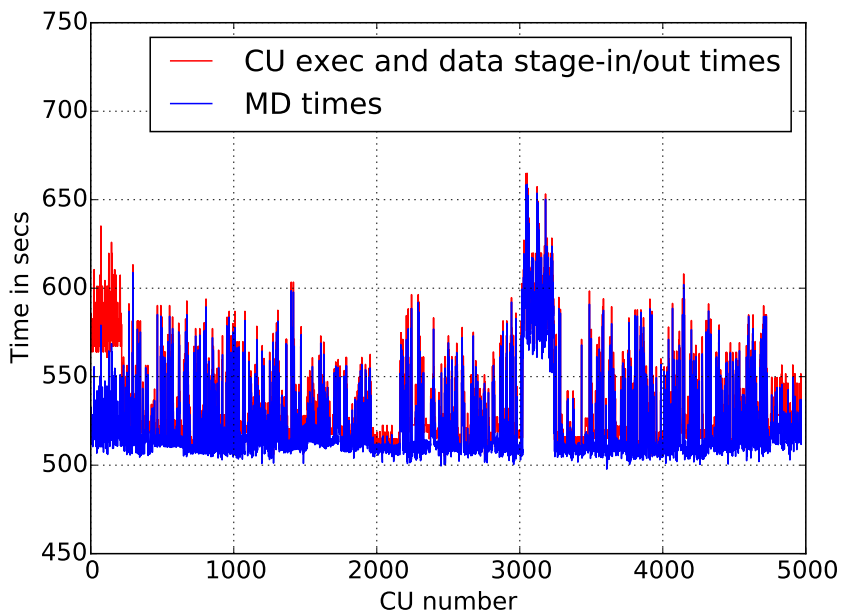


Figure 8.9: Execution times for MD tasks when running QM/MM REMD with synchronous RE pattern and using **216** replicas: times to run Amber (sander) executable (blue line); times to run Amber executable plus times for file staging (red line). For all simulation runs all replicas are running concurrently. All runs are performed on Stampede HPC cluster.

Results of the simulation run with 1000 replicas are depicted in Figure 8.11. In contrast to two previous runs, file staging times are now much larger (red bars). For some units file staging times can be as long as 50 seconds. At the same time, fluctuation in execution time is very similar to what we have previously observed.

Finally we present execution times for simulation run with 1728 replicas. As shown in Figure 8.12, for the first 1728 Compute Units file staging times are substantially longer. In some cases, file staging takes more than 100 seconds. The main reason for this behavior is the setup of the shared file system on Stampede. For the rest of the Compute Units, file staging times are larger than before, but not by a significant amount. In addition, in this simulation run, there is a single Compute Unit (nr. 10003), for which execution time, is much larger than for all other units. This is not uncommon for QM/MM simulations, where some replicas might not even finish the certain number of simulation time-steps within simulation time limits.

We have quantified and measured fluctuation in execution times for REMD QM/MM simulations with various replica counts. Our experiments demonstrate, that for these simulations there is scope for improvement in resource utilization. We have also investigated how file staging times are varying as the simulation progresses and the number of replicas is increased. For all runs, file staging times for the first set of units are substantially longer than for the rest of the

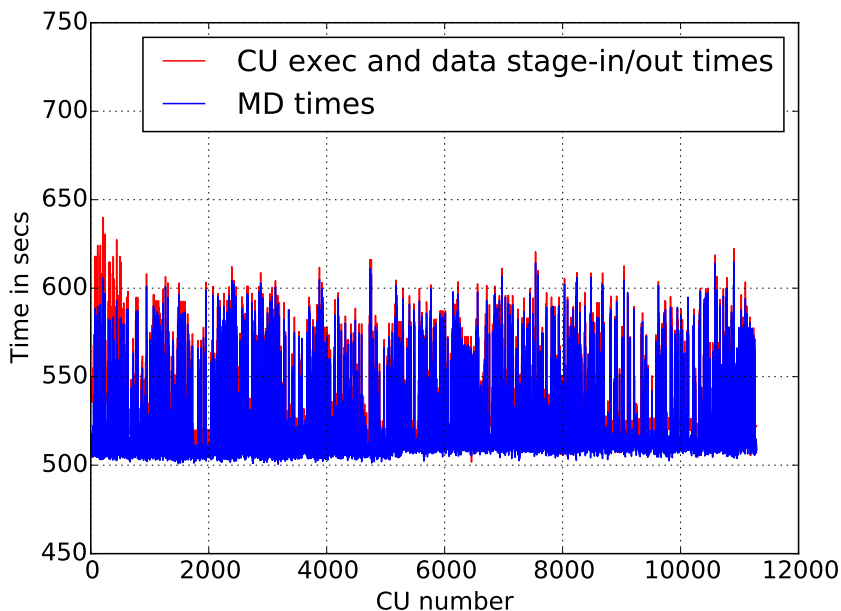


Figure 8.10: Execution times for MD tasks when running QM/MM REMD with synchronous RE pattern and using **512** replicas: times to run Amber (sander) executable (blue bars); times to run Amber executable plus times for file staging (red bars). For all simulation runs all replicas are running concurrently. All runs are performed on Stampede HPC cluster.

units. This is caused by the creation and staging of restraint files during the first simulation cycle and setup of the shared file system on Stampede. For subsequent simulation cycles, the longest file staging times were observed for the run with 1000 replicas (up to 40 seconds).

To compare resource utilization of synchronous and asynchronous RE pattern we perform simulation runs with 215, 512, 1000, 1728 replicas, while varying the number of simulation time-steps between exchanges from 2000 to 500. Results of these runs are presented in Figure 8.13.

As shown in Figure 8.13, for all numbers of simulation time-steps, increase in the number of replicas results in decrease in resource utilization.

### 8.6.2 Exchange phase

To understand how exchange phase is affected by the RE pattern (synchronous or asynchronous) we examine the number of crosswalks, the number of accepted exchanges and the number of attempted exchanges for 1D temperature exchange REMD. Here crosswalk is calculated for each replica and is defined as a transition from the current state to every other available state. In other words, a given replica has to exchange temperature with every other replica. A crosswalk takes at least  $N$  (number of replicas) simulation cycles.

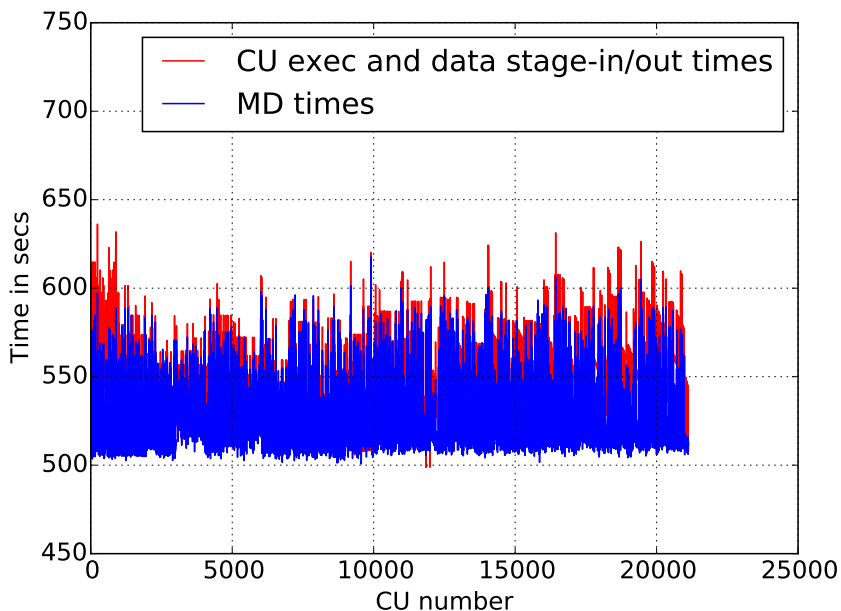


Figure 8.11: Execution times for MD tasks when running QM/MM REMD with synchronous RE pattern and using **1000** replicas: times to run Amber (sander) executable (blue bars); times to run Amber executable plus times for file staging (red bars). For all simulation runs all replicas are running concurrently. All runs are performed on Stampede HPC cluster.

We again use alanine dipeptide and for all simulation run we perform 6000 time-steps between exchanges. All simulation runs are performed on SuperMIC HPC cluster. For all runs we set the range of temperatures from 300 to 460 degrees. All runs are performed under weak scaling scenario, where each replica is run on a single CPU core and we perform runs with 40, 80 and 160 replicas. Each run takes 480 minutes in real time.

For asynchronous RE, we denote a ratio of replicas, which have to finish MD phase before entering an exchange phase, to the total number of replicas as  $w$ .

For this simulation setup, there is no fluctuation in execution times for MD tasks and asynchronous RE pattern doesn't have any advantage in terms of performed simulation time. Despite that, this simple simulation setup enables us to investigate how the choice of synchronization mechanism affects exchange metrics.

### Number of crosswalks

In Figure 8.15 are plotted crosswalk values for both RE patterns. As we can see, for synchronous pattern, increase in the number of replicas results in increase in the number of crosswalks. This behavior is expected, since we keep the range of temperatures the same (from 300 to 460) for all runs, which means that for runs with larger number of replicas difference in temperatures

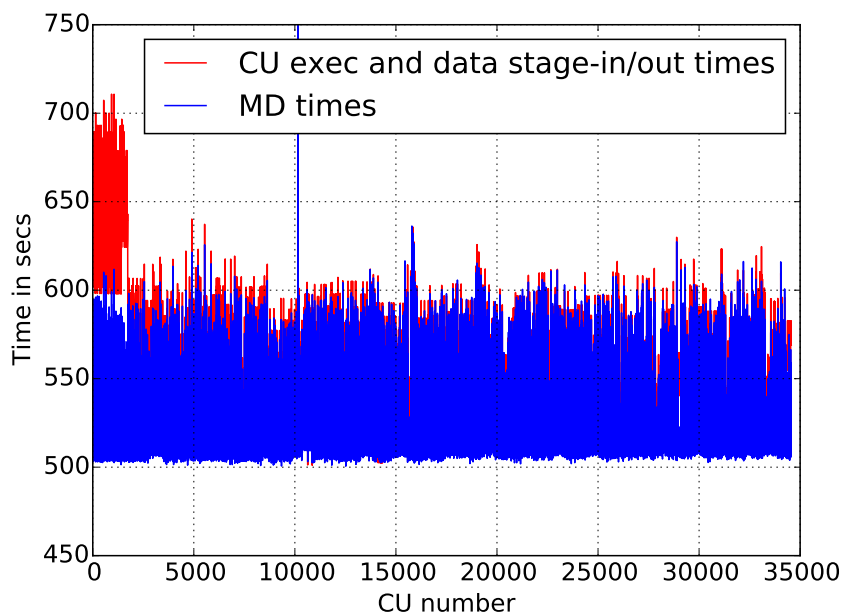


Figure 8.12: Execution times for MD tasks when running QM/MM REMD with synchronous RE pattern and using **1728** replicas: times to run Amber (sander) executable (blue bars); times to run Amber executable plus times for file staging (red bars). For all simulation runs all replicas are running concurrently. All runs are performed on Stampede HPC cluster.

between neighboring replicas is smaller.

### Number of accepted exchanges

Next, we demonstrate the number of accepted exchanges for the same set of simulation runs (Figure 8.16).

### Number of attempted exchanges

Finally, in Figure 8.17 we plot attempted exchanges.

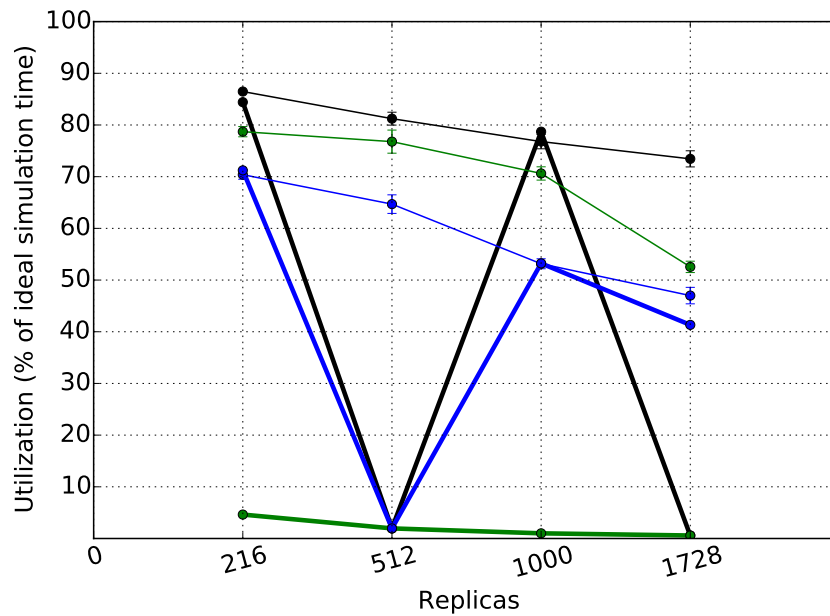


Figure 8.13: Utilization for asynchronous and synchronous RE patterns using different replica counts. Utilization is a percentage of maximal (ideal) simulation time.

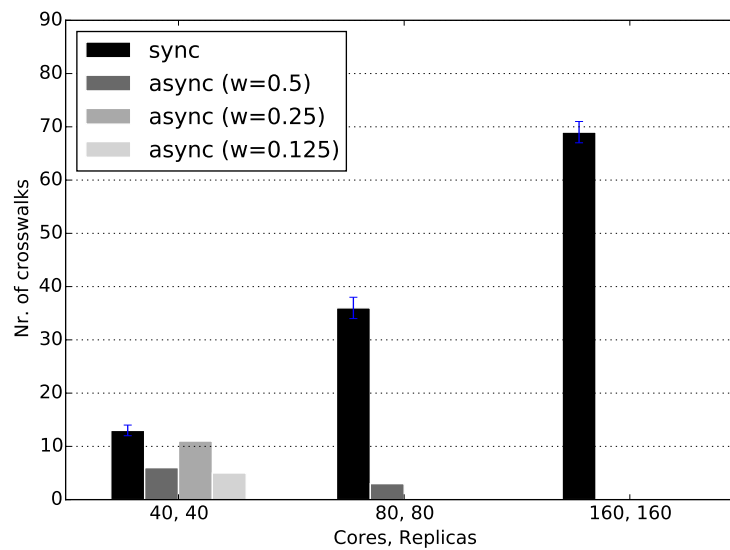


Figure 8.14: Number of crosswalks for 1D T-REMD with synchronous and asynchronous RE patterns. All runs performed on SuperMIC cluster. Runs with synchronous RE pattern (black bars), asynchronous RE pattern with  $w = 0.5$  (dark gray bars) and asynchronous RE pattern with  $w = 0.1$  (light gray bars)

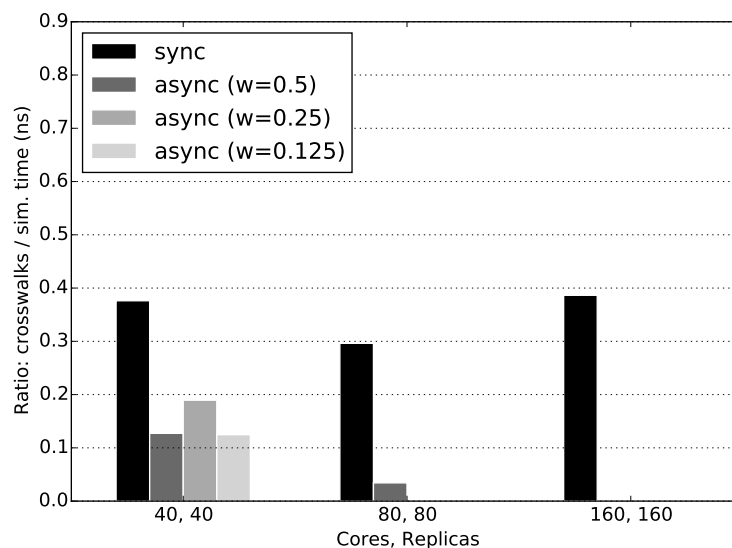


Figure 8.15: Ratio of crosswalks to simulation time (ns) for 1D T-REMD with synchronous and asynchronous RE patterns. All runs performed on SuperMIC cluster. Runs with synchronous RE pattern (black bars), asynchronous RE pattern with  $w = 0.5$  (dark gray bars) and asynchronous RE pattern with  $w = 0.1$  (light gray bars)

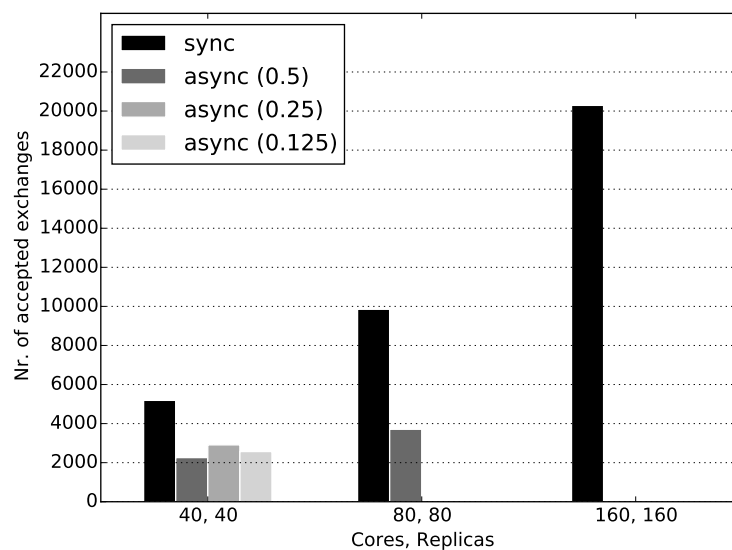


Figure 8.16: Number of accepted exchanges for 1D T-REMD with synchronous and asynchronous RE patterns. All runs performed on SuperMIC cluster. Runs with synchronous RE pattern (black bars), asynchronous RE pattern with  $w = 0.5$  (dark gray bars) and asynchronous RE pattern with  $w = 0.1$  (light gray bars)



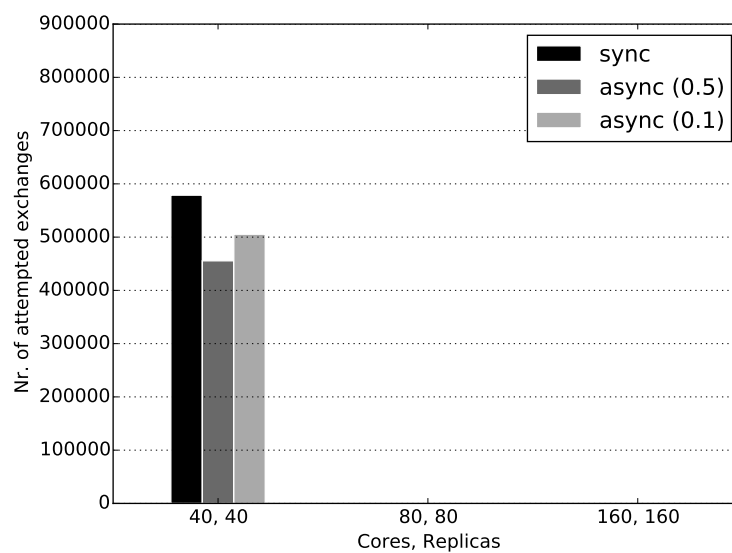


Figure 8.17: Number of attempted exchanges for 1D T-REMD with synchronous and asynchronous RE patterns. All runs performed on SuperMIC cluster. Runs with synchronous RE pattern (black bars), asynchronous RE pattern with  $w = 0.5$  (dark gray bars) and asynchronous RE pattern with  $w = 0.1$  (light gray bars)

## Chapter 9

### Analysis

RepEx was designed to address functional, performance and usability requirements outlined in Chapter ???. In Chapter ??, we demonstrated capabilities of RepEx and characterized its performance for 1D and 3D REMD simulations. We saw the range of exchange parameters that it supports and the flexibility in their ordering (e.g., TUU versus TSU). Furthermore we demonstrated RepEx supporting Amber and NAMD MD engines with minimal conceptual or implementation changes.

We saw the ability to utilize different RE patterns and Execution Modes, which is made available by decoupling exchange parameters (T/U/S), dimensionality and algorithm (sync. vs. async.) from the resource management and execution details. As such, it is accurate to say that RepEx satisfies the functional and usability requirements.

Most of the recent developments of molecular simulation software packages for Replica Exchange, are developed with aim to demonstrate ability to efficiently utilize computational resources at large scales and/or using large number of replicas. While these developments provide new scientific insights and are advancing the field of molecular simulation software, they often are tightly coupled with a particular setup.

First, software is developed for a particular HPC cluster and is targeting a specific hardware configuration. This means that the code is not portable and it is unlikely that demonstrated results will be achieved on another supercomputer. We could adopt a similar approach and develop a highly scalable code for a specific HPC cluster. While this is not a trivial exercise, it's usefulness is questionable. Instead, our aim was to develop a software package which is capable of demonstrating high scalability and performance on variety of HPC clusters.

Second, development can be done with a particular RE algorithm in mind. Performance results in this case can be attributed to infrequent communication pattern or small amount of data, which is sent during the exchange. It is important to ensure, that REMD software not only supports different RE algorithms, but also demonstrates good scalability and performance results for these algorithms.

	<b>Amber</b>	<b>Gromacs</b>	<b>LAMMPS</b>	<b>VCG async</b>	<b>CHARMM</b>	<b>Charm++/ NAMD MCA</b>	<b>RepEx</b>
Max replicas	~2750	~900	100	240	4096	2048	3584
Max CPU cores	~5490	~150000	76800	1920	131072	524288	13824
Fault tolerance	n/a	n/a	n/a	basic	n/a	n/a	basic
MD engines	Amber	Gromacs	LAMMPS	IMPACT	CHARMM	NAMD	Amber, NAMD
RE patterns	sync	sync	sync	sync, async	sync	sync	sync, async
Nr. Exec. Modes	1	1	1	2	1	1	2
Nr. dims	2	2	2	2	2	2	3
Exchange params	3	2	2	2	2	2	3

Table 9.1: Comparison of molecular simulation software packages with integrated REMD capability. We characterize each of the seven packages based on 8 features. For each feature we provide a numerical value or a name corresponding to that feature.

In Table 9.1, we have summarized the most important features of seven existing packages used for REMD, some of which are used by communities of hundreds, if not thousands of users. In this table, we have included three popular MD simulation engines, namely Amber, LAMMPS and Gromacs that have been extended to provide RE capabilities and four REMD packages that have been designed to be external to MD engines.

For each feature we have provided numerical value of that feature. The only exception is MD engines, where we have provided actual engine name.

As can be seen from Table 9.1, a majority of the packages are designed to address a subset of features we identified as necessary to be flexible and general purpose. Many packages have eschewed generality for performance. For example, Charm++/NAMD MCA package can utilize  $O(100,000)$  cores but does not provide flexible resource utilization nor asynchronous exchange capabilities. On the other hand, VCG RE package is one of the few packages, which supports asynchronous RE but it has limited scalability (both in the number of replicas and CPU cores) and is tightly coupled to IMPACT which is not an open source MD engine. Similar to most other existing solutions, both VCG and Charm++/NAMD are limited in the number of exchange parameters as well as in flexibility in the ordering of exchange parameters.

Clearly a balance between performance and functional requirements needs to be maintained. On the evidence of Table 9.1 we believe that RepEx provides an optimal balance. As evidenced

by the rigorous requirements analysis, design and implementation considerations, RepEx embodies the sound systems engineering principles along with software engineering practices. RepEx has been used for algorithmically innovative molecular science simulations [21]. For example, when simulating a non-enzymatic transesterification reaction using QM/MM, preliminary results with asynchronous RE pattern, demonstrate higher utilization values in comparison with synchronous RE pattern. Utilization is defined as a percentage of ideal resource utilization, when CPUs are used only to perform MD. Importantly, in the case of asynchronous pattern, sampling quality is not compromised due to execution of replicas in groups, in each of the three dimensions.

## Chapter 10

### Conclusion

In this thesis we have introduced RepEx – a highly flexible python package, which supports the scalable execution of user configurable multi-dimensional REMD simulations on a variety HPC resources. We have shown that RepEx can achieve respectable performance and scalability on various HPC systems, including petascale machines such as Stampede.

The two core design features of RepEx are: the separation of MD simulation engine from the implementation of RE algorithm; the use of a pilot system as a runtime, which separates the algorithm and workload management from the resource management and runtime complexity.

As a consequence of the former, the integration of new MD simulation engines is significantly simplified and facilitates the reuse of RE patterns and Execution modes. We believe that this also lowers the barrier for development and testing of new REMD algorithms. As a consequence of the second design principle, our implementation decouples execution specifics from the REMD algorithm and enables users to choose from the multiple execution options. Collectively, this allowed us to introduce the concept of Replica Exchange patterns, which can be used interchangeably. To the best of our knowledge none of the currently available REMD implementations have this capability.

The range of scalability (performance), generality (independent of MD engine) and flexibility (different configurations of exchanges) as demonstrated in the experiments validates the design of RepEx.

## Chapter 11

### Future Work

There are planned several extensions to the RepEx framework:

- Internal implementation of the single point energy calculations for salt concentration exchange
- Addition of the new exchange parameters, such as pH, to enable support for new types of multi-dimensional REMD simulations.
- Support for other MD simulation engines
- Explicit support for the simulations concurrently utilizing multiple HPC resources

## Bibliography

- [1] “Protein data bank.” <http://www.rcsb.org/pdb/home/home.do>, accessed: 2015-11-11.
- [2] J. C. Phillips, R. Braun, W. Wang, J. Gumbart, E. Tajkhorshid, E. Villa, C. Chipot, R. D. Skeel, L. Kale, and K. Schulten, “Scalable molecular dynamics with namd,” *J. Comput. Chem.*, vol. 26, no. 16, pp. 1781–1802, 2005.
- [3] R. H. Swendsen and J.-S. Wang, “Replica monte carlo simulation of spin-glasses,” *Physical Review Letters*, vol. 57, no. 21, p. 2607, 1986.
- [4] Y. Sugita and Y. Okamoto, “Replica-exchange molecular dynamics method for protein folding,” *Chemical physics letters*, vol. 314, no. 1, pp. 141–151, 1999.
- [5] H. Fukunishi, O. Watanabe, and S. Takada, “On the hamiltonian replica exchange method for efficient sampling of biomolecular systems: application to protein structure prediction,” *The Journal of chemical physics*, vol. 116, no. 20, pp. 9058–9067, 2002.
- [6] Y. Meng and A. E. Roitberg, “Constant ph replica exchange molecular dynamics in biomolecules using a discrete protonation model,” *J. Chem. Theory Comput.*, vol. 6, no. 4, pp. 1401–1412, 2010.
- [7] R. Salomon-Ferrer, D. A. Case, and R. C. Walker, “An overview of the amber biomolecular simulation package,” *Wiley Interdisciplinary Reviews: Computational Molecular Science*, vol. 3, no. 2, pp. 198–210, 2013. [Online]. Available: <http://dx.doi.org/10.1002/wcms.1121>
- [8] S. Pronk, S. Páll, R. Schulz, P. Larsson, P. Bjelkmar, R. Apostolov, M. R. Shirts, J. C. Smith, P. M. Kasson, D. van der Spoel *et al.*, “Gromacs 4.5: a high-throughput and highly parallel open source molecular simulation toolkit,” *Bioinformatics*, vol. 29, no. 7, pp. 845–854, 2013.
- [9] “Repex on github,” <https://github.com/radical-cybertools/radical.repex>, accessed: 2015-11-11.
- [10] A. Merzky, M. Santcroos, M. Turilli, and S. Jha, “RADICAL-Pilot: Scalable Execution of

- Heterogeneous and Dynamic Workloads on Supercomputers,” 2015, (under review) <http://arxiv.org/abs/1512.08194>.
- [11] Y. Sugita, A. Kitao, and Y. Okamoto, “Multidimensional replica-exchange method for free-energy calculations,” *The Journal of Chemical Physics*, vol. 113, no. 15, pp. 6042–6051, 2000.
  - [12] D. J. Earl and M. W. Deem, “Parallel tempering: Theory, applications, and new perspectives,” *Physical Chemistry Chemical Physics*, vol. 7, no. 23, pp. 3910–3916, 2005.
  - [13] N. Rathore, M. Chopra, and J. J. de Pablo, “Optimal allocation of replicas in parallel tempering simulations,” *The Journal of chemical physics*, vol. 122, no. 2, p. 024111, 2005.
  - [14] A. Kone and D. A. Kofke, “Selection of temperature intervals for parallel-tempering simulations,” *The Journal of chemical physics*, vol. 122, no. 20, p. 206101, 2005.
  - [15] H. Yu and L. Kale, “Scalable molecular dynamics with namd on the ibm blue gene/l system,” 2008.
  - [16] W. Jiang, Y. Luo, L. Maragliano, and B. Roux, “Calculation of free energy landscape in multi-dimensions with Hamiltonian-exchange umbrella sampling on petascale supercomputer,” *J. Chem. Theory Comput.*, vol. 8, pp. 4672–4680, 2012.
  - [17] B. R. Brooks, C. L. Brooks, A. D. MacKerell, L. Nilsson, R. J. Petrella, B. Roux, Y. Won, G. Archontis, C. Bartels, S. Boresch *et al.*, “Charmm: the biomolecular simulation program,” *J. Comput. Chem.*, vol. 30, no. 10, pp. 1545–1614, 2009.
  - [18] W. Jiang, J. C. Phillips, L. Huang, M. Fajer, Y. Meng, J. C. Gumbart, Y. Luo, K. Schulten, and B. Roux, “Generalized scalable multiple copy algorithms for molecular dynamics simulations in namd,” *Computer physics communications*, vol. 185, no. 3, pp. 908–916, 2014.
  - [19] W. Shalongo, L. Dugad, and E. Stellwagen, “Distribution of helicity within the model peptide acetyl (aaqaa) 3amide,” *Journal of the American Chemical Society*, vol. 116, no. 18, pp. 8288–8293, 1994.
  - [20] B. K. Radak, M. Romanus, E. Gallicchio, T.-S. Lee, O. Weidner, N.-J. Deng, P. He, W. Dai, D. M. York, R. M. Levy, and S. Jha, “A Framework for Flexible and Scalable Replica-Exchange on Production Distributed CI,” ser. XSEDE ’13, 2013, pp. 26:1–26:8.



- [21] B. K. Radak, M. Romanus, T.-S. Lee, H. Chen, M. Huang, A. Treikalis, V. Balasubramanian, S. Jha, and D. M. York, "Characterization of the Three-Dimensional Free Energy Manifold for the Uracil Ribonucleoside from Asynchronous Replica Exchange Simulations," *Journal of Chemical Theory and Computation*, vol. 11, no. 2, pp. 373–377, 2015, <http://dx.doi.org/10.1021/ct500776j>. [Online]. Available: <http://dx.doi.org/10.1021/ct500776j>
- [22] J. L. Banks, H. S. Beard, Y. Cao, A. E. Cho, W. Damm, R. Farid, A. K. Felts, T. A. Halgren, D. T. Mainz, J. R. Maple *et al.*, "Integrated modeling program, applied chemical theory (impact)," *J. Comput. Chem.*, vol. 26, no. 16, pp. 1752–1780, 2005.
- [23] J. Xia, W. F. Flynn, E. Gallicchio, B. W. Zhang, P. He, Z. Tan, and R. M. Levy, "Large-scale asynchronous and distributed multidimensional replica exchange molecular simulations and efficiency analysis," *J. Comput. Chem.*, vol. 36, pp. 1772–1785, 2015.
- [24] M. P. Allen and D. J. Tildesley, *Computer simulation of liquids*. Oxford university press, 1989.
- [25] S. Kullback and R. A. Leibler, "On information and sufficiency," *The annals of mathematical statistics*, pp. 79–86, 1951.
- [26] E. Gallicchio, M. Lapelosa, and R. M. Levy, "Binding energy distribution analysis method (bedam) for estimation of protein- ligand binding affinities," *J. Chem. Theory Comput.*, vol. 6, no. 9, pp. 2961–2977, 2010.
- [27] C. Bergonzo, N. M. Henriksen, D. R. Roe, J. M. Swails, A. E. Roitberg, and T. E. Cheatham III, "Multidimensional replica exchange molecular dynamics yields a converged ensemble of an RNA tetranucleotide," *J. Chem. Theory Comput.*, vol. 10, pp. 492–499, 2014.
- [28] M. T. Panteva, T. Dissanayake, H. Chen, B. K. Radak, E. R. Kuechler, G. M. Giambasu, T.-S. Lee, and D. M. York, *Multiscale Methods for Computational RNA Enzymology*. Elsevier, 2015, ch. 14.
- [29] B. Ensing, M. De Vivo, Z. Liu, P. Moore, and M. L. Klein, "Metadynamics as a tool for exploring free energy landscapes of chemical reactions," *Acc. Chem. Res.*, vol. 39, no. 2, pp. 73–81, 2006.

- [30] E. Vanden-Eijnden, “Some recent techniques for free energy calculations,” *J. Comput. Chem.*, vol. 30, no. 11, pp. 1737–1747, 2009. [Online]. Available: <http://dx.doi.org/10.1002/jcc.21332>
- [31] T. Dissanayake, J. M. Swails, M. E. Harris, A. E. Roitberg, and D. M. York, “Interpretation of pH-Activity Profiles for Acid-Base Catalysis from Molecular Simulations,” *Biochemistry*, vol. 54, pp. 1307–1313, 2015.
- [32] J. T. Mościcki, “Diane-distributed analysis environment for grid-enabled simulation and analysis of physics data,” in *Nuclear Science Symposium Conference Record, 2003 IEEE*, vol. 3. IEEE, 2003, pp. 1617–1620.
- [33] I. Raicu, Y. Zhao, C. Dumitrescu, I. Foster, and M. Wilde, “Falkon: a fast and light-weight task execution framework,” in *Proceedings of the 2007 ACM/IEEE conference on Supercomputing*. ACM, 2007, p. 43.
- [34] A. Casajus, R. Graciani, S. Paterson, A. Tsaregorodtsev *et al.*, “Dirac pilot framework and the dirac workload management system,” in *Journal of Physics: Conference Series*, vol. 219, no. 6. IOP Publishing, 2010, p. 062049.
- [35] A. Luckow, M. Santcroos, A. Merzky, O. Weidner, P. Mantha, and S. Jha, “P: a model of pilot-abstractions,” in *E-Science (e-Science), 2012 IEEE 8th International Conference on*. IEEE, 2012, pp. 1–10.
- [36] J. B. Swadling, D. W. Wright, J. L. Suter, and P. V. Coveney, “Structure, dynamics, and function of the hammerhead ribozyme in bulk water and at a clay mineral surface from replica exchange molecular dynamics,” *Langmuir*, vol. 31, no. 8, pp. 2493–2501, 2015.
- [37] M. Turilli, M. Santcroos, and S. Jha, “A Comprehensive Perspective on Pilot-Jobs,” 2015, <http://arxiv.org/abs/1508.04180>.
- [38] “Extreme science and engineering discovery environment,” <https://www.xsede.org/resources/overview>, accessed: 2015-11-11.
- [39] T.-S. Lee, B. K. Radak, A. Pabis, and D. M. York, “A new maximum likelihood approach for free energy profile construction from molecular simulations,” *J. Chem. Theory Comput.*, vol. 9, pp. 153–164, 2013.
- [40] T.-S. Lee, B. K. Radak, M. Huang, K.-Y. Wong, and D. M. York, “Roadmaps through free energy landscapes calculated using the multidimensional vFEP approach,” *J. Chem. Theory Comput.*, vol. 10, pp. 24–34, 2014.

- [41] “Repex experiments,” <https://github.com/radical-cybertools/radical.repex/blob/master/EXPERIMENTS.md>, accessed: 2015-11-11.

## Appendix A

### Appendix

#### A.1 Abbreviations

- **Target/Remote system** - HPC cluster which user can access via communication network and which is used to execute simulation tasks
- **Local system** - laptop or desktop to which user has physical access
- **Pilot** - task-container launched on compute nodes of HPC cluster and executing tasks according to their description
- **Simulation phase** - first phase of REMD simulation, during which replicas propagate MD simulation. Simulation phase can be defined as a number of time-steps, e.g. 2 ps or as a fixed real time period, e.g. 1 minute
- **Exchange phase** - second phase of REMD simulation, during which replicas exchange thermodynamic parameters.
- **Simulation Cycle** - simulation phase followed by exchange phase for 1D-REMD and M simulation phase, exchange phase pairs for M-REMD
- **Task** - a unit of execution. There is a one-to-one mapping between tasks and RP's Compute Units.
- **Total Simulation Time** - total time required to perform **N** Simulation Cycles
- **Replica Exchange Pattern** - REMD simulation type definition based on synchronization mode between simulation and exchange phases
- **Execution Mode** - a set of execution options decoupling simulation requirements from the resource availability and enabling flexible usage of allocated CPU's on HPC resources
- **Bulk submission** - all tasks of a current step are submitted at once (as a Python list) to RADICAL-Pilot for execution - `unit_manager.submit_units(tasks)`

- **Sequential submission** - tasks of a current step are submitted sequentially, one by one to RADICAL-Pilot for execution
- **RP overhead** - task launching delay on a target resource and communication delay
- **RepEx overhead** - task preparation time, e.g. association of data and parameters with a task and translation of task description to RP task description (creation of Compute Units); time to perform RepEx method calls inside simulation loop on a local system

## A.2 I/O patterns for different types of REMD simulations with Amber MD engine

In this section we present and discuss file movement patterns for three exchange types supported for the use with Amber MD engine: Temperature exchange, Umbrella exchange and Salt Concentration exchange. Understanding the file movement requirements for a particular exchange type is a fundamental step in enabling efficient and scalable implementation. It is important to point out, that despite being similar, file movement patterns for different exchange types have some important differences. We only discuss file movement patterns for one-dimensional simulation types, since file movement in any multi-dimensional simulation is a sequential concatenation of one-dimensional patterns.

For all three file movement patterns simulation is decomposed into five stages - initialization, MD simulation, individual exchange, global exchange and post processing. Intuitively, initialization is performed on a local system. At this stage simulation input files are identified according to the user input. MD simulation stage is done on a remote system. This stage requires as an input a set of input files transferred from a local system and other files which are generated dynamically on a remote system, just before the MD simulation. Individual exchange is a part of the exchange phase, which can be performed concurrently by multiple processing units. A subset of MD simulation output files is used as an input for individual exchange stage. Contents of this subset depend on the exchange type. For all three exchange types the output of the individual exchange stage is a single file - `matrix.column.dat`. As the name suggests, each of these files contains a single column of the Gibbs "swap" matrix, which is used during the exchange procedure. For global exchange stage are required all `matrix.column.dat` files, which are used to compose a swap matrix. Global exchange stage is responsible for the majority of exchange calculations. This stage as an output produces a single file - `exchange.pairs.dat`.

In this file are provided id's of the pairs of replicas, which must exchange their respective parameters. Finally, `exchange_pairs.dat` file is transferred back to the local system, where actual exchange of parameters is performed enabling generation of the next set of Compute Units for MD simulation.

We first present a file movement pattern for Temperature exchange, then for Umbrella exchange and finally for Salt Concentration exchange.

### A.2.1 Temperature exchange

File movement pattern for temperature exchange simulation is depicted in Figure ?? . Initialization stage requires a user to specify at least three shared input files: parameters file (`.prmtop`), input file template (`.mdin`) and coordinates file (`.inpcrd`). These files are required as in input of the MD simulation stage. In addition to these three files, just before the MD simulation stage is generated a simulation input file `init_input.mdin`. Starting with second simulation cycle, instead of initial input coordinates file, MD simulation stage requires as input a restart file of the previous cycle - `restart_id.c.rst`. After the MD simulation stage are generated four files: `output.mdout`, `trajectory.mdcrd`, `restart_id.c.rst` (is used as an input for the next cycle) and `history.mdinfo`. The latter file is required as an input of the individual exchange stage. It is important to note that each individual exchange task requires a `history.mdinfo` of each replica in it's group. That is if we perform an individual exchange calculations for replica with  $id = 1$  and the group to which this replica belongs is  $G = \{1, 2, 3, 4\}$ , then `history.mdinfo` files of replicas 1, 2 and 4 are required as input for individual exchange of replica 1. As mentioned previously individual exchange for each replica produces a `matrix.column.dat` file. Which is required as input for the global exchange stage. The global exchange stage, in turn produces a single `exchange_pairs.dat` file, which is used for local post-processing.

### A.2.2 Umbrella exchange

In Figure A.2.2 is presented a file movement pattern for umbrella exchange simulations. In addition to parameters file (`.prmtop`), input file template (`.mdin`) and coordinates file (`.inpcrd`), initialization stage requires user to specify a restraints template file (`.RST`). Before MD simulation stage, this file is used to generate an individual restraints (`restraint.RST`) file for each replica. In addition to the files specified for MD simulation stage of the temperature exchange file movement pattern, umbrella exchange requires two extra files: restraints template file `rstr.template.RST` and `restraint.RST`. Similarly as for temperature exchange,

first simulation cycle of MD stage requires `init_coors.inpcrd` file, but subsequent cycles must use `restart_id.c.rst` of the previous cycle. Individual exchange stage, as an input takes two files: `history.mdinfo` file for current replica and `restraint.RST` for all replicas in current group. As an output of the individual exchange stage is generated a single `matrix_column.dat` file. File requirements of global exchange and post-processing stage are identical with temperature exchange pattern described above.

### A.2.3 Salt Concentration exchange

I/O pattern for salt concentration exchange is shown in Figure A.2.3. As we can see, I/O for initialization stage and MD simulation stage is exactly the same as for temperature exchange. For salt concentration exchange, individual exchange is more involved than for other REMD types and consists of three steps. First is `pre_exec` step, where `inp_energy.mdin` files for Amber's group execution are generated. Next step is actual execution, where single point energies for replicas in current group are calculated. This step produces `inp_energy.mdinfo` files as an output. The final step of the individual exchange stage is `post_exec`. In this step, single point energies from the `inp_energy.mdinfo` files for all replicas in the current group are read-in and is produced a `matrix_column.dat` file. Global exchange and post processing stages are exactly the same as for other REMD types.

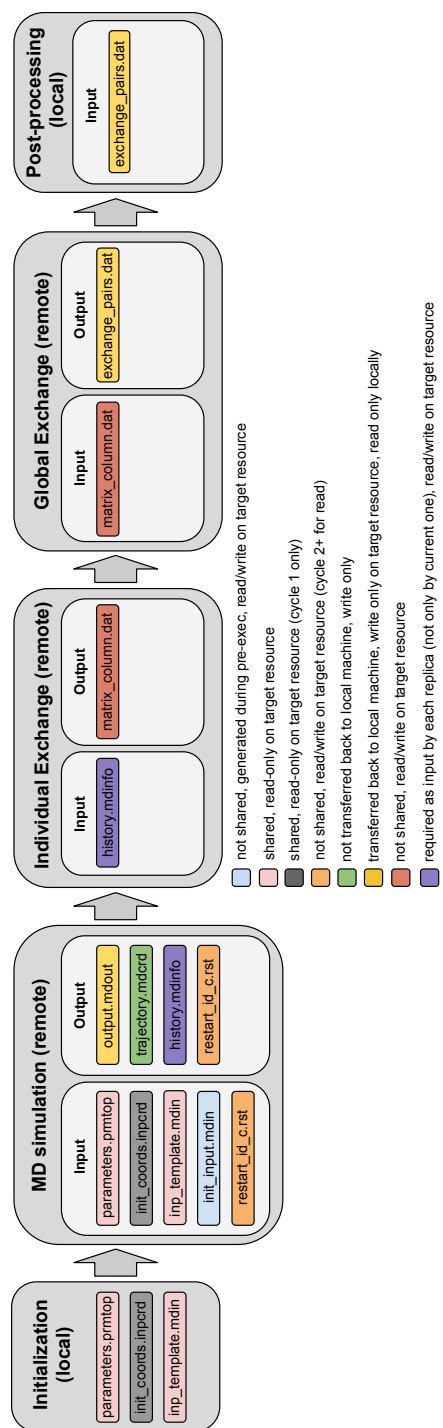


Figure A.1: File movement pattern for Amber MD engine: Temperature exchange.



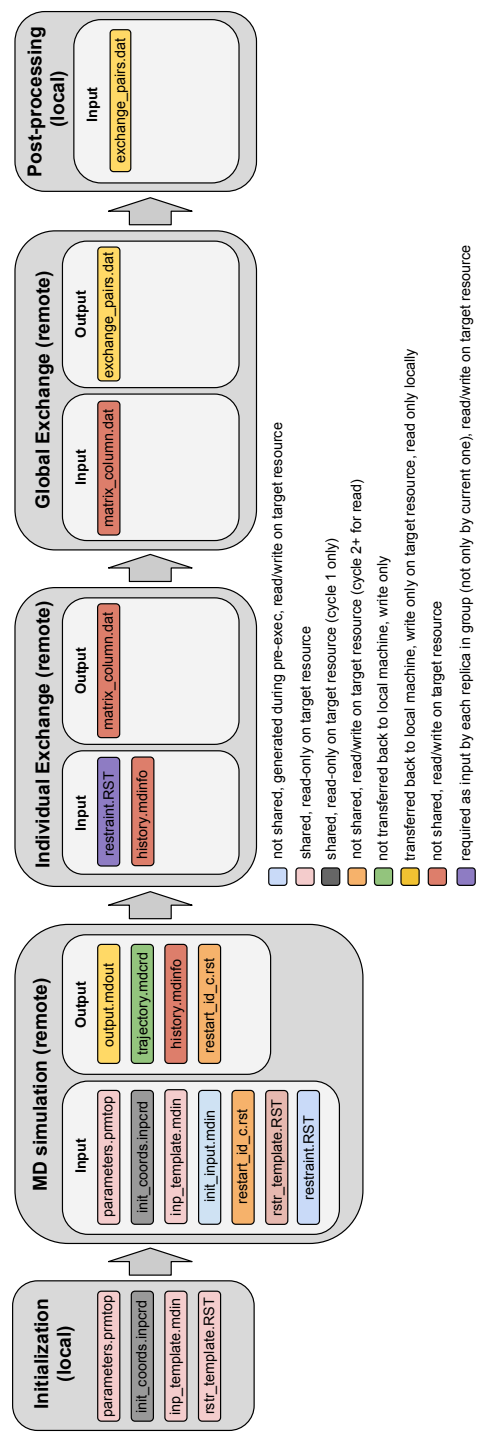


Figure A.2: File movement pattern for Amber MD engine: Umbrella exchange.

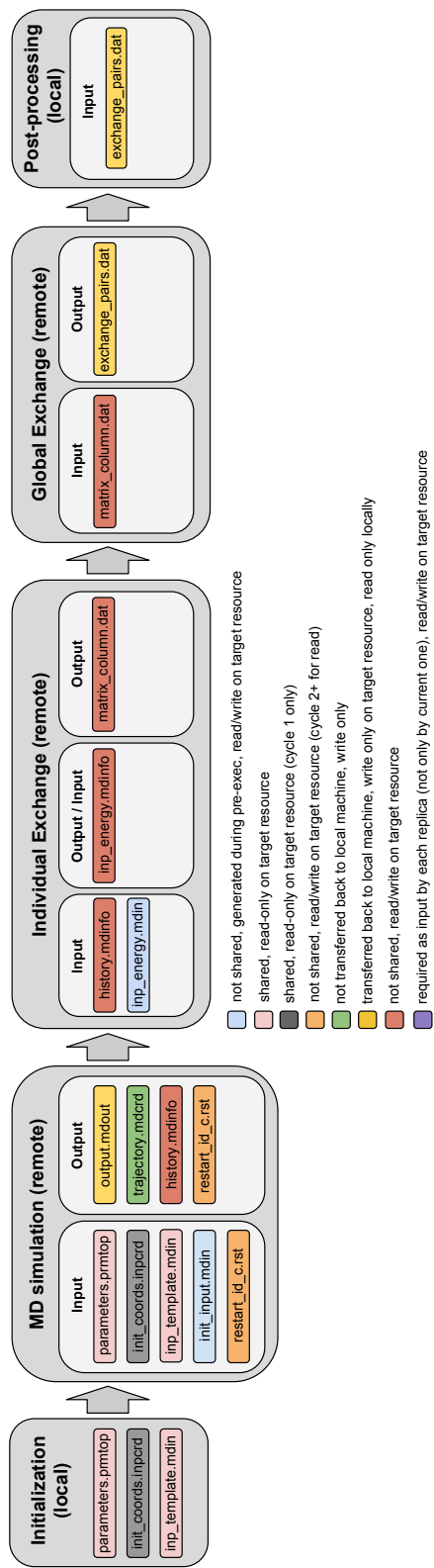


Figure A.3: File movement pattern for Amber MD engine: Salt Concentration exchange.